Declaration

I, Luo Sigang, declare that this thesis titled,

"A Proposal of a Stationary Wireless Power Transmission System in Electrical Trains and a Sensorless Positioning Control of On-board Coils
電気鉄道の静止形非接触集電システムの提案と車上コイルの位置センサレス補正"

and the work presented in it are my own. I confirm that:

❖ This work was done wholly or mainly while in candidature for a research degree at this University.
❖ Where any part of this thesis has previously been submitted for a degree or any other qualification at this University or any other institution, this has been clearly stated.
❖ Where I have consulted the published work of others, this is always clearly attributed.
❖ Where I have quoted from the work of others, the source is always given. With the exception of such quotations, this thesis is entirely my own work.
❖ I have acknowledged all main sources of help.
❖ Where the thesis is based on work done by myself jointly with others, I have made clear exactly what was done by others and what I have contributed myself.

Signed:_____

Date:_____

Acknowledgement

First and foremost, I want to say thanks to My supervisor Professor Koseki Takafumi, the best teacher I have met in my life, form the bottom of my heart. Honestly speaking, I was always a trouble student who made a lot of mistakes and brought problems to him, but he always teaches me patiently in a gentle way, encourages me when I feel frustrated and gives me a lot of help in daily life. Therefore, I respect him not only as a professor, but also a father in Japan. As my supervisor, he always teaches me to be active and think in a more logical way. Unfortunately, I understood it very late, but now I start to know how valuable his instructions are. I will always regard him as an example both in my future work and life.

Deepest thanks and apologize to Tamura Riya and her family. Everything started from here and it is impossible for me to adjust myself to life in Japan with their help.

Then, I want to express deep thanks to Takada san for his help in life and guide in experiment. As a foreign student, it is hard for me to find some stores in Japan, so he always brought for me. And I will never forget the movement he came back from Akihabara with my MCU in hot summer. Thank you very much!

Thank Matsusaki san, the secretary of our lab, her existing makes this lab lively.

Also, I want to show my thanks to Professor Kondo and all other members in our WPT group from Chiba University, they gave me a lot of instructions in my experiment.

Then, I want to thank all the members from Koseki lab for their help. It is an excellent lab but I am not an excellent student, thus I received much more help than I can provide in these past two years. I want to thank all of you, thank Shoichiro senapi, Art san, Didier, Duc san, Guo, Matsuoka, Narita, Salman, Miura, Takeda and Shimoda for your valuable advice and priceless accompany. And here are special thanks to Valerio, who told me conclusion should always be first; to Shin san, who showed me what is hard working; to Duc san, who always makes me think I am a fool when discussing with him; to Didier, who always complains together with me about boring things and plays with me. All of you are nice guys, and wish all of us a brighter future.

Thank Carol.Liu, for many things, thank you very much.

Finally I want to show my thanks to my family, who always support me and give me confidence. Love you forever.

Abstract

This paper studies WPT system for electrical trains. It discusses about the current drawbacks of using catenary&pantograph system for railway power supplying and mentions the merits of using WPT as a solution.

About stationary WPT system, this paper mentions one of the biggest problems for its stable and efficient operation, that is coil misalignment. Then presents a coil position control system which can be used in railway applications, as a solution.

For this coil position control system, as sensorless method to detect the position of coils is presented, which also shows a strong tolerance to vertical deviation of gap. As the result, the presented system is able move coils to the expected position with error less than 6.25% coil length, when gap deviation happens within -50%~+100%.

Structure of this paper is shown below:

Chapter 1 is introduction, it talks about the drawbacks of current power supply system based on catenary&pantograph at first, then points out the merits of applying WPT technology to railway system. About WTP technology, history and classification are introduced briefly, also the most suitable one for railway application is selected. Then, two methods used for railway system is introduced and problems of them are stated. Finally, the research motivation of this research is shown.

Chapter 2 shows the configuration of current stationary WPT system for railway application. Then shows what kind of misalignment will occur in such system and how will such misalignment affect system performance.

Chapter 3 analyzes the characteristic of electromagnetic field when misalignment happens, and then presents a sensorless detection method for coil positioning. To improve the system robustness against gap deviation, a method to eliminate affect of gap deviation is also presented .

Chapter 4 is the part of experiment, it verifies the method proposed in chapter 3 by controlling linear actuator to move the coil to aligned position. By setting the coils under different gap deviation conditions, the method to improve system robustness is also verified.

Chapter 5 is conclusions and future works.

Content

Chapter 1--Introduction

This chapter talks about the drawbacks of current power supply system based on catenary&pantograph at first, then points out the merits of applying WPT technology to railway system. About WTP technology, history and classification are introduced briefly, also the most suitable one for railway application is selected. Then, two methods used for railway system is introduced and problems of them are stated. Finally, the research motivation of this research is shown.

1.1 Background

1.1.1 Drawbacks of current railway power supply system with catenary

Nowadays, power supply system based on catenary&pantograph is applied in most of the railway systems, as in Fig_1.1.1. Basically this system is able to supply power to trains stably and safely with high efficiency. However, with the passing of time, it has been proved that this system also has some drawbacks, as following:

Fig_1.1.1 Power supply system based on catenary [1]

1. Obstacle to city view

From Fig_1.1.1, even the catenary are carefully arranged. Large amount of power supply wire and pole still make it looks mess, and this problem will be more serious in a tourism city or historic city. Thus it is not friendly to sight seeing.

2. Safety risks

The pole can be injured or damaged by some external causes such as extreme weather and earthquake. Fig_1.1.2 shows an accident happened in Yamanote Line, a busy commuting line for many people. The pole is worn due to aging and pulled down by the force from the wire. This accident caused 9 hours suspension of running and affected the schedule of about 410,000 in different degrees. Also, in some narrow cities, such catenary will be set near residential buildings, which brings risk of touching by little children.

3. Maintenance cost

In this system, power is transfer by physical contact between pantograph and catenary, friction between them will also accelerate the aging. In order to avoid accident from aging, frequent maintenance have to be ensured, which increases the cost as a result.
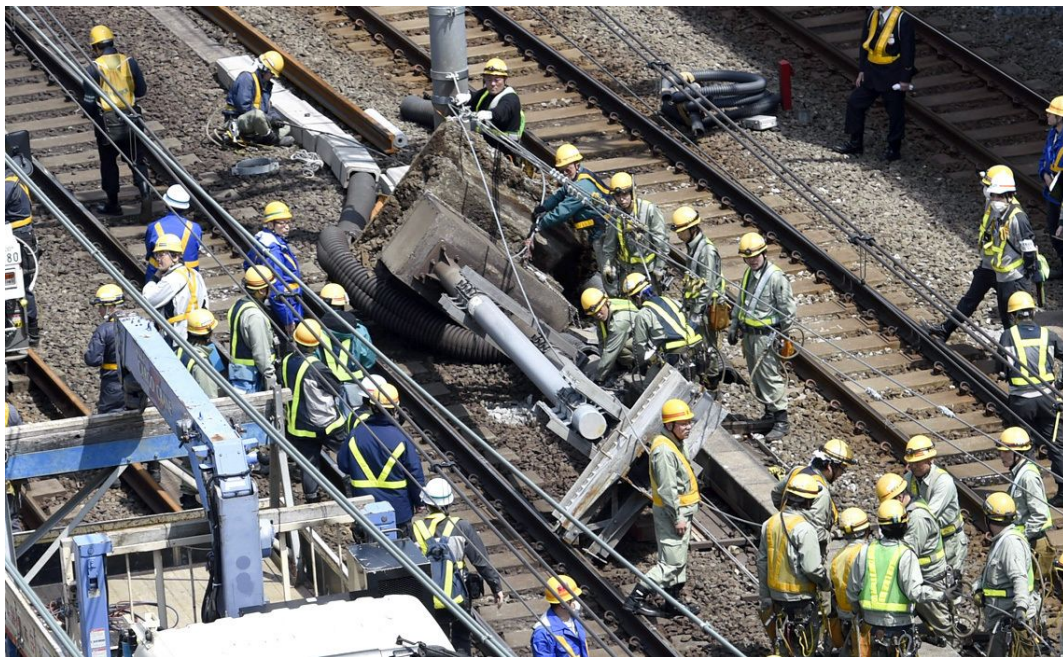
Fig_1.1.2 Accident of catenary system [2]

1.1.2 Merits of using Wireless Power Transmission (WPT) system

Drawbacks of using catneary&pantograph system for power charging have been discussed above. Actually, not only railway system, many transportation systems, especially public transportation systems are facing the similar problems. Therefore, a new method which can transmit power without catenary are proposed, and it is called

Wireless Power Transmission (WPT). Wireless means there is no wire used when power is transmitted form power transmitter to power receiver. Also, because there is no physical contact between power transmitter and receiver, this technology is also called as Contactless Power Transfer (CPT). In this paper, only WPT will be used to avoid confusing. Fig_1.1.3 shows how this technology is used in several transportation systems.

From this comparison, if WPT is applied into transportation system, view obstacles will be eliminated, safety risks such as touched by little children will be removed, charging will become more convenient and robustness to extreme weather will be improved. As a result, all city beauty, human safety, charging convenience and system economical can be improved.
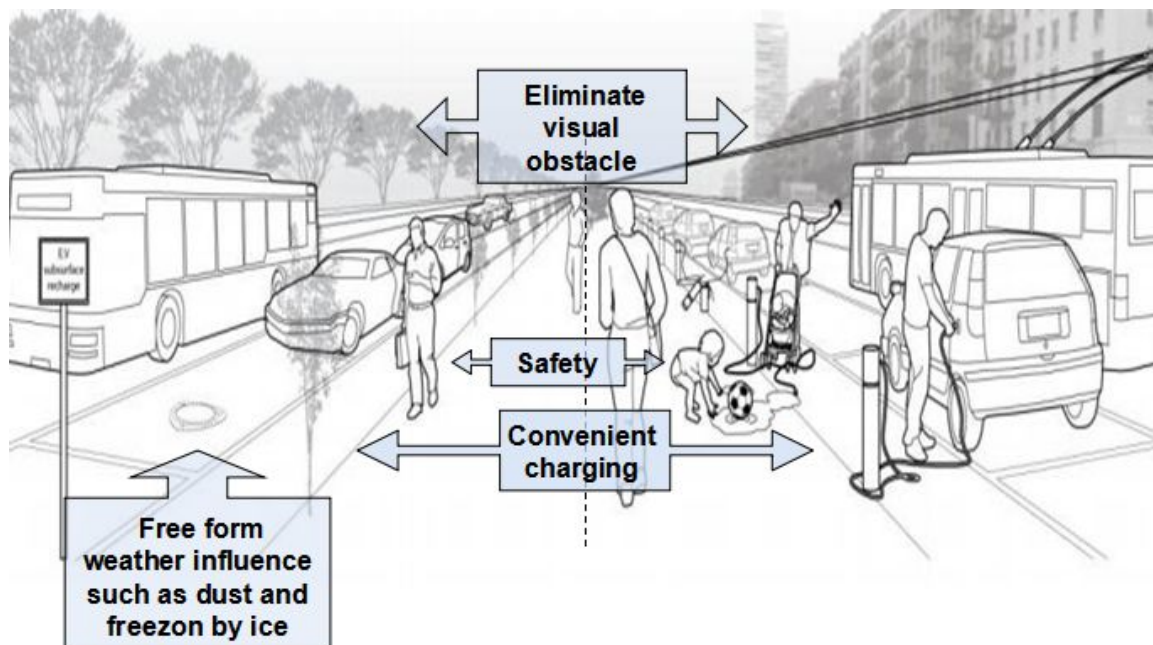
Fig_1.1.3 Comparison of transportation system (left) based on WPT and (right) catneary&wire system[3]

1.2 Introduction of WPT technology

Section 1.1 mentioned the drawbacks of current catenary&pantograph system used for railway and explained the merits of applying WPT system in transportation systems. Thus, the concept of wireless power transfer will be introduced and which WPT method is the most suitable one for railway will be discussed.

### 1.2.1 History and classification of WPT technology

Although many types of WTP technology are existing today, they have a common ancestor--Nikola Tesla, the man who performed the first experiment in wireless power transmission. He experimented with transmitting power by inductive and capacitive

coupling using spark-excited radio frequency resonant transformers, now called "Tesla Coils", with high generated AC voltage[4]. Also by using an enormous coil to generate voltages of the order of 10 mega-volts, three incandescent lamps at a distance of about one hundred feet were lighted by him[5]. But for long-range and high power charging, even Tesla claimed his ideas were proven, experiment was not successful, there is no concrete evidence which can prove that he ever transmitted significant power besides the short-range demonstrations above[4].

After Nikola Tesla, little progress was made in WPT during a long period. Although radio was developed for communication, it is not suitable for WPT because low-frequency radio waves spreads out in all directions.

In past decades, significant improvement of WPT starts with William C.Brown, who created rectenna and converted microwave to DC power efficiently, this was verified by his model helicopter powering experiment[6].

And nowadays, existing WPT technology can be roughly classified as far-field WPT, which mainly includes microwave and laser, and near-field, which mainly include inductive coupling and magnetic resonance. Comparison of these four technologies is shown in Fig_1.2.1. And detailed explanations are as following:
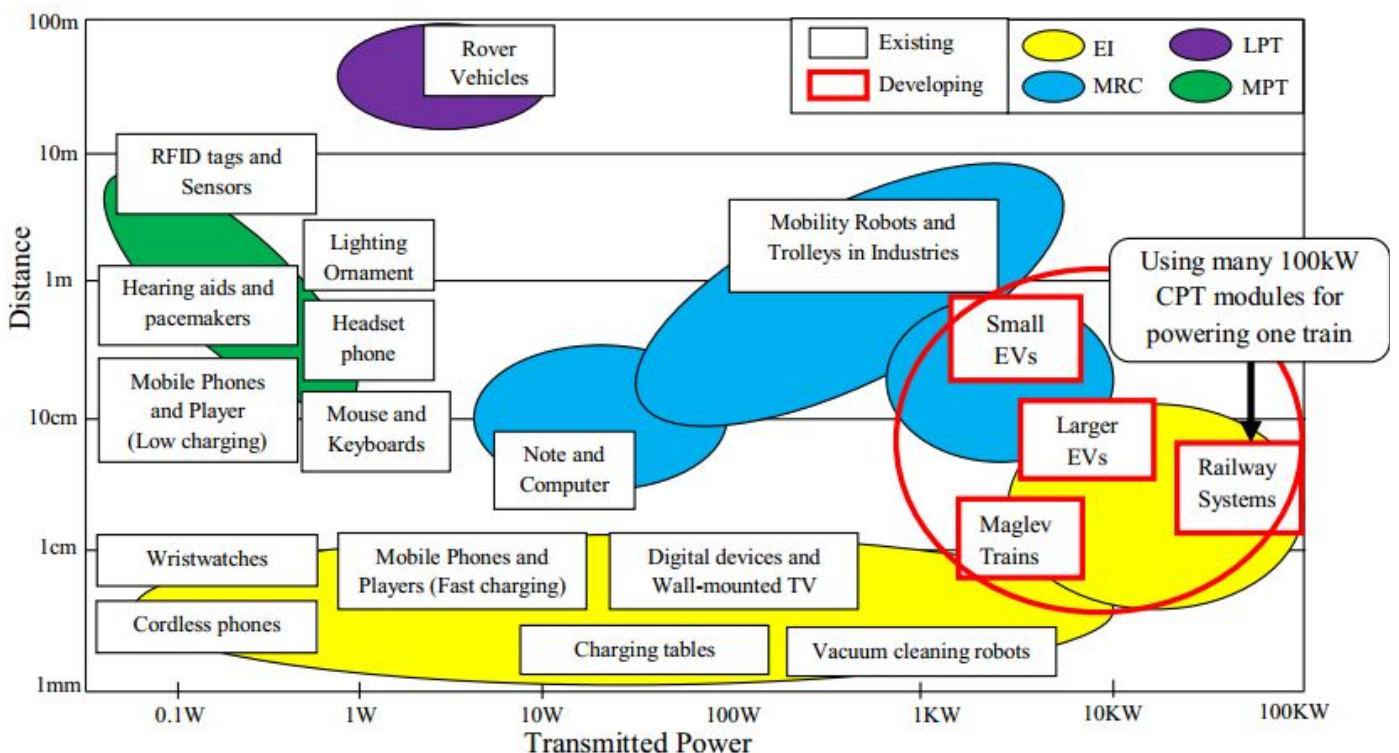
Fig_1.2.1 Comparison of WPT methods [7]

EI--Electromagnetic Inductive; MRC--Magnetic Resonance Coupling;
LPT--Laser Power Transfer; MPT--Microwave Power Transfer

Far-field
1. Microwave Power Transfer(MPT):
   This technology mainly transmits power at frequency-level of GHz, power beaming using microwave can reach the distance from sever to hundreds kilometers, which means far-field. By using rectenna, converting microwave energy to electricity power has been realized at 95% efficiency[8]. Limitation of this technology is the necessity of extremely larger power transmitter and receiver, because the human safe power density of this technology is only 1mW/(cm)^2. This method is mainly proposed to transmit power to spacecraft of gathering power from solar power satellites[9][10].
2. Laser Power Transfer (LPT):
   This technology transmits power by converting electricity into a laser beam which is then pointed at a photovoltaic cell. Working frequency of this method can reach THz, much higher than microwave. This technology has notable merit such as very large transmitting distance and high access control ability, due to its extremely high frequency. But it also has obvious demerits, laser radiation is hazardous to human and energy conversion from light and electricity is still low, about 40%-50%. This technology is mainly explored in military weapons and aerospace, commercial use of this technology have to follow strict safety criteria

Near-field
1. Inductive Power Transfer (IPT)
   Inductive coupling, also called as Electromagnetic Induction (EI), Inductive Coupling (IC). As oldest one among all WTP methods, it is also the most widely used one in commercial applications. Power is transferred between coils by a magnetic field. Transmitter and receiver form a losely coupled transformer[11][12]. Cores are used to improve the coupling coefficient, like a normal transformer. Compered with far-field WPT method, this technology can transmit large power (kW) at high efficiency(>90%). By using resonant circuit, power can be transmitted to farther places, but still within the range of about several diameter of coil[11]. Commercial applications of this method ranges from medical device implemented in human body to vehicles such as Electrical Vehicle (EV) and trains[13][14][15][16].
2. Magnetic Resonance (MR)
   This method is also called "Resonant Inductive Coupling", and critically speaking, it is some kind of mid-field WPT, because it has larger distance than inductive coupling, about 4~10 coil diameter. Drawbacks of this method when compared with inductive coupling is smaller power range and power splitting phenomenon at short distance. This method is explored to build area wireless power covered area such as a wireless room to power small devices, and also to supply power to private EV and small buses[17][18].

In railway application, requirement of transmitting is only several dozen centimeter, but requirement of power is high to drive the heavy vehicle. From above comparison, Electromagnetic Induction will be the one fits railway best. Actually, EI is selected by most of the existing railway system which use WPT technology, such as KAIST from Korea and Bombardier form Canada[19][20][21][22].

## 1.2.2 Railway power supply system based on WPT

Railway system based on WTP can be classified into two classes: dynamic charging and stationary charging (also called as static charging)[23]. They are shown as follows:

Dynamic charging:
This system charges the vehicle continuously while vehicle is running. Fig_1.2.2 shows the "Primove Rail" proposed by Bombardier based on IPT technology. In dynamic charging system, since power is transferred all the time, requirement of power transfer ability can be reduced. Therefore, in this system only cables are used as primary transmitter to save system cost. At secondary, flat ferrite core and coil are used as power pick-ups(receiver). This system has strong tolerance to misalignment, a serious problem in WPT technology which will be explained in chapter 2, thus efficiency can also be ensured. But this merit of it also brings drawback to this system, long primary side leads to more cost for primary side. Though only using cable can reduce the cost of power transmitter, required amount of inverters and maintenance fee will be increased proportional to the distance of whole line. The dynamic charging system developed by KAIST[24] (Fig_1.2.3) has the similar problem as well.
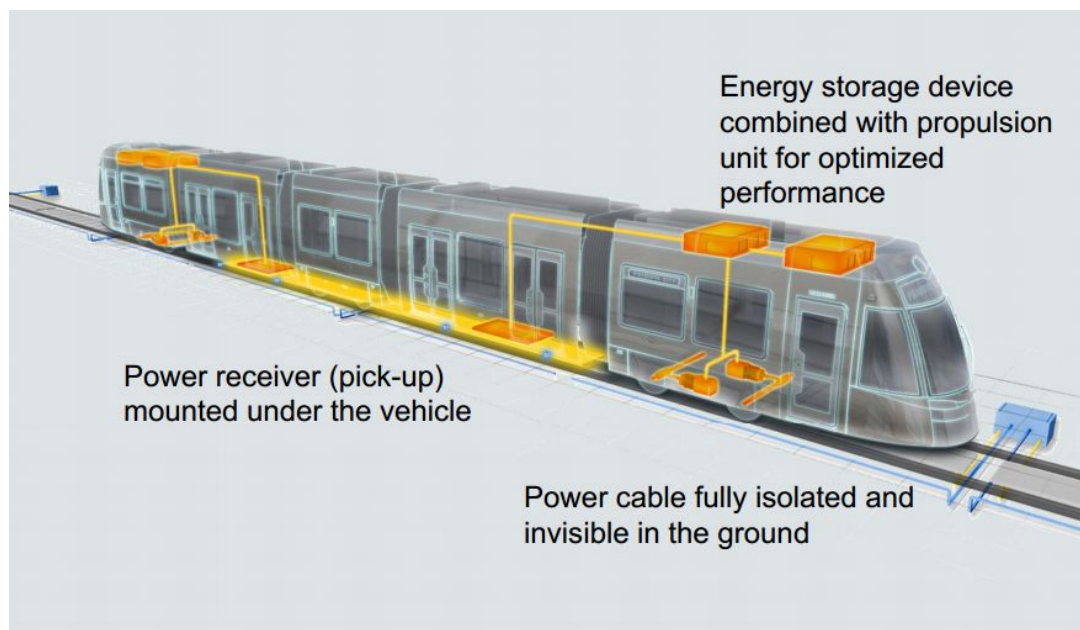
Fig_1.2.2 Primove from Bombardier [22]
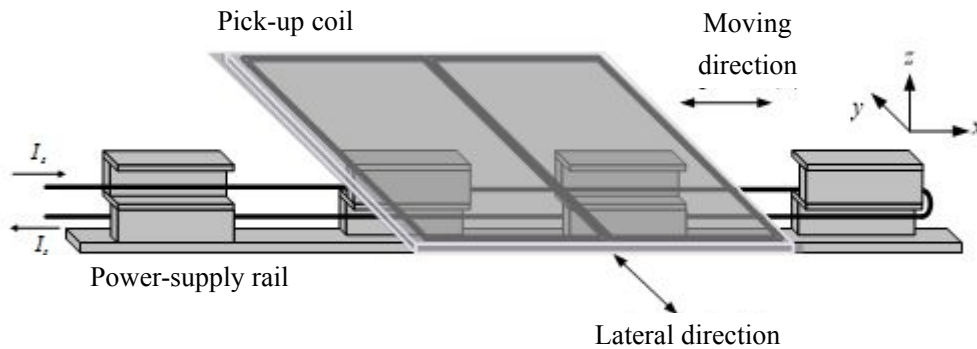
Fig_1.2.3 Power transmitter and receiver developed by KAIST [24]

Stationary charging system:

Unlike dynamic charging system, this system only charge the vehicle when it stops in station or at charging point. Obviously, this system can reduce construction and maintenance cost of primary power transmitting system. By using the combination of ferrite core and coils, power transfer capacity is improved and much higher than dynamic charging system. However, unlike dynamic system, misalignment of coils in the moving direction of train will happen when it stops, due to the relatively inaccurate stop position of train. And this will be the problem to be solved in this paper.

1.3 Research motivation

1.3.1 Related researches about coil misalignment

Coil misalignment is one of the most important reasons which make it hard to apply stationary WPT to commercialization in railway system. Therefore many researches are made and try to solve this problem. And they can be roughly classified as coil shape designing, inverter/converter controlling and vehicle positioning.

For inverter/converter controlling, S.Kitazawa proposed a control method of power converter in 2013 [25]. In this method, an instantaneous current control method is applied to the PWM rectifier. Secondary current flows though the load is detected and used to calculate the voltage over the load, and this voltage can be used as feedback and compared with the reference voltage. Thus a closed-loop control of power is built. This method is able to ensure the power transfer capacity until the mutual inductance starts to drop quickly. Thus controllable range in this system is only about 25% of core length. If this is applied to railway system which uses 80 cm core, the controllable range of misalignment will be about 20 cm, which is not enough if larger misalignment happens.

In another study of control method, S.Aldhaher presents a method to electronically

tune a Class E inverter used as a primary coil driver in an inductive WPT system to minimize the affect of misalignment in 2014 [28]. The tuning method uses current controlled inductors and a variable switching frequency to achieve optimum switching conditions. However, similar as the method in [25], performance of the system can only be ensured before coupling coefficient starts to drop fast, which means the performance can not be always ensured.

For coil shape designing. In 2005, Nishimura form Yokohama National University has proposed a system with longer primary coils and shorter secondary coil to increase the overlapped area between them [26]. This method makes the system stable, but the longer primary coil also brings large leakage of flux. Therefore, the average efficiency is low, which is not economical and not suitable for commercial use. C.Zheng also proposed a system with smaller secondary core and larger primary in 2014 [31]. It is not suitable for our system for the same reason.

Similar to Nishimura, T.Gerrits proposed a system consists of three secondary coils and one primary coil in 2011 [29]. And the total length of secondary coils is longer than the primary. This system will choose one or two secondary coils which have the best coupling condition to transfer the power. Thus it can transfer power stability at large misalignment distance. This system has higher However, in railway system the space on train is limited, thus there will not be enough space for too many extra coils.

Method of adding repeater between primary and secondary coil to extend available charging range, proposed by T.Imura in 2011 [30], this method is mainly designed for creating a WPT environment. Because the lack of space for repeater coil, this method is not suitable for train system.

And all the methods mentioned above have a common drawback. No matter if the core shape is changed or inverter/converter is controlled, the physical characteristic of coil coupling condition at misaligned position is not changed, which means these method are only useful when magnetic field changes within small range. Also, such controlling and shape designing will bring higher switching lose or lower average efficiency, more or less. Therefore, they can not totally solve the problem.

For such reason, some studies are made to detect and control coil position, however they are mainly designed for EV and not suitable for railway application. The details are as follows:

Grant A.Covic proposed a system to detect relative position of coils for dynamic charging system of EV in 2014 [31]. In this system, two extra detection coils are used at primary side to detect the existing of passing secondary coil. It is not suitable for railway for two reasons. Firstly, this system only detect whether there is secondary coil before primary but not the precise position, which is not enough for position control. Secondly, this system uses extra detection coils, which increases system cost.

For coil self-positioning. Palakon proposed a automatic stop system for EV[18]. This system can guide the EV to stop at the right position. But it also has some drawbacks when applied to railway system. First, this system starts the positioning when EV is approaching the charger, which means the direction is known at first. However, unlike a EV which only has one couple of transmitting and receiving coil, a train has much more couples of coil. If the detection starts before trains, there is

possibility that transmitting coil and receiving coil are not from the same couple are used for positioning, which will lead to error. Also, controlling train position is more complex and inaccurate when compared with controlling EV position, which means extra device should be used to control the position of coils.

1.3.2 Problem statement

Finally, as analyzed above, in this paper the author try to solve the following problems:

(1) Only designing the core shape or control method of inverter can not eliminate the problem of misalignment, because of the physical limitation of poor coupling condition is still existing. So it is necessary to design a stationary WPT system which can eliminate misalignment effect by controlling coil position.

(2) Sensorless positioning method can help system save cost. But for train system, we need to design a method which can detection coil position when coils are static.

Chapter 2--Proposal of a Railway Power Supply System based on Stationary WPT

This chapters shows the configuration of current stationary WPT system for railway application. Then shows what kind of misalignment will occur in such system and how will such misalignment affect system performance.

2.1 System configuration and requirements

2.1.1 System configuration
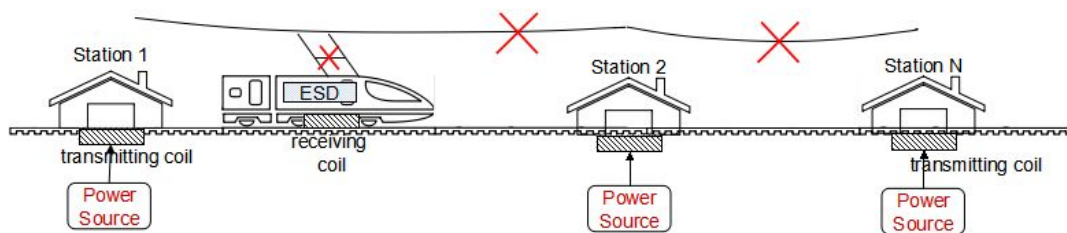
Fig_2.1.1 System configuration

About the operation of such system, power is charged during dwelling time of the train and used to drive the motor during the running time of train. Also, regenerated power will be stored during the deceleration time before train stops. Based on such operation, at least two merits can be obtained:

(1) **Costing saving:** since power supply system is only implemented in stations, construction cost and maintenance fee can be saved.
(2) **Energy saving:** since regenerative power is restored by the train itself, more energy will be saved.

To achieve such operation. System shown in Fig_2.1.1 is built. Instead of using suspended catenary, power are supplied by the transmitting coils installed in each station. Power receiving coils are installed on the train to replace the pantograph, thus a complete power transmitting and receiving system is built. Also, since power is only transmitted during the dwelling time of train, Energy Storage Devices (ESD) are also needed to restore the power for motor driving. Both battery and supper capacitor can be selected for such purpose. Fundamentally, power transmitting&receiving system and storage system make up the stationary WPT system of electrical trains.

2.1.2 Basic requirements of system

For the effective and efficient operation of such system, following requirements should be satisfied:

(1) Charging capacity: large charging capacity is required to power the train running from one station to the next, since dwelling time of train is relatively short, generally less than 1 min and most are about 30~40 seconds, charging power should be relatively high. In Light Rail Transit (LRT) condition, required charging capacity for is about 100 kW.

(2) Charging stability: variation of charging power should be limited within acceptable range. When power is too high, over current will be generated over the ESD and make it overheated. On the other hand, when power is too low, charging will be failed, thus energy stored in the ESD will be not enough to power the train to the next station.

(3) Charging efficiency: low efficiency means unfriendly to environment and uneconomical, thus high efficient is a basic requirement for most charging systems.

## 2.2 Problems of coil misalignment in stationary WPT of railway application

2.2.1 Affect of coil misalignment on power charging

Misalignment of coils will affect the power charging performance greatly. And this section will show the numerical analysis of such affect.

Fig_2.2.1 shows the detailed configuration of the system shown in section 2.1. In the dot line block is the power transmitter at primary side and power receiver at secondary side. They make up a contactless transformer, which can be expressed by using the equivalent circuit in Fig_2.2.2.
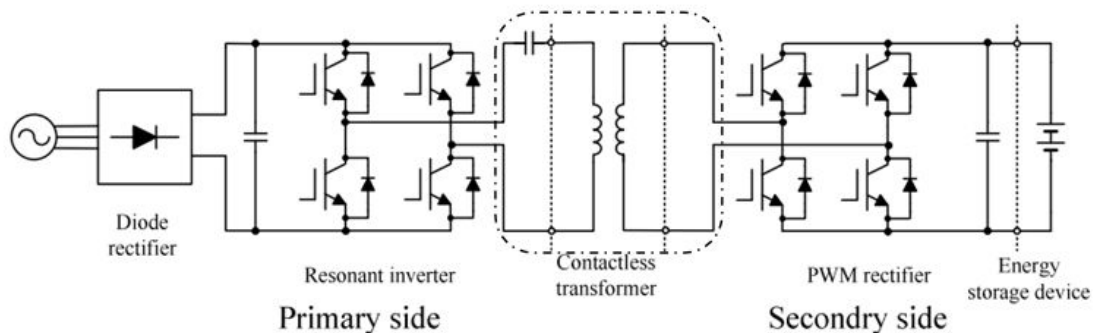
Fig_2.2.1 Detailed configuration of stationary WPT system [25]
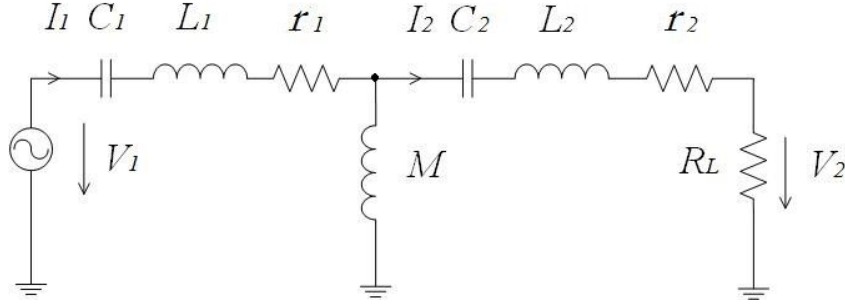
Fig_2.2.2 Equivalent circuit of contactless transformer

Part outside the frame is the topology of power source $V1$, load RL and capacitors $C1=C2$, which are used to compensate the reactive power generated by leakage inductance. If the frequency of power source is ω, $C1$ and $C2$ will be calculated as eq(2-1) to make the system resonant.

$$C_1 = C_2 = \frac{1}{\omega^2(L_1+M)} \tag{2-1}$$

Part inside the frame is the transformer itself. $r1=r2$, $L1=L2$ and they represent the resistors and leakage inductance of primary and secondary sides, respectively. Xm is mutual inductance, through which power is transferred.

Then, eq(2-2)~eq.(2-7) can be obtained as follows:

In primary side:

$$V_1 = j\omega(M+L_1)I_1 + I_1r_1 - j\frac{1}{\omega C_1}I_1 - j\omega MI_2 \tag{2-2}$$

In secondary side:

$$j\omega MI_1 = I_2r_2 + j\omega(M+L_2)I_2 + I_2R_L - j\frac{1}{\omega C_2}I_2 \tag{2-3}$$

Impedance $Z1$ and $Z2$ are defined :

$$Z_1 = j(\omega L_1 + \omega M - \frac{1}{\omega C_1}) + r_1 \tag{2-4}$$

$$Z_2 = j(\omega L_2 + \omega M - \frac{1}{\omega C_2}) + r_2 \tag{2-5}$$

Power over RL :

$$P_L = I_2^2 R_L \approx \frac{V_1^2\omega^2 M^2}{(Z_1 R_L + \omega^2 M^2)^2}R_L \tag{2-6}$$

Efficiency η:

$$\eta = \frac{I_2^2 R_L}{\mathrm{Re}(V_1 I_1)} \tag{2-7}$$

Then, power and efficiency at each misaligned position is calculated by using the module in Fig_3.3.1 and Tab_3.3.1. Here RL is 950 Ω, which can be used to transfer 100kW when coil is at the aligned position. Calculation result is shown in Fig_2.2.3.

From this result, power received by ESDwill increase fast and reach maximum 160% when misalignment reaches 150 mm, and then decreases until it becomes 0 at 400 mm misalignment. According to the discussion in section 2.1.2, charging capacity can not be ensure at large misalignment and charging stability can not be ensured at small misalignment. Therefore, misalignment of coils make the performance of system unreliable.
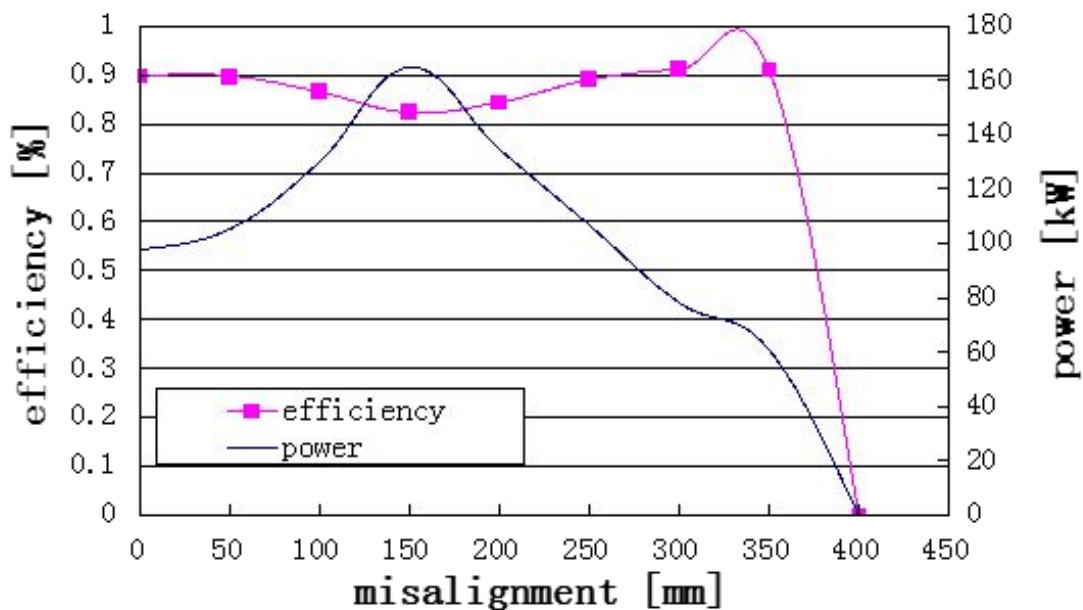
Fig_2.2.3 Effect of misalignment on power charging performance

2.2.2 Misalignment in railway system

After discussing the affect of misalignment. This section will discuss the misalignment phenomenon in railway condition.

Obviously, since the vehicle runs on the rail, misalignment at left and right side of the train will not happen. However, because of the inaccurate stopping position of train, misalignment in the moving direction will happen.

Nowadays most trains are stopped manually by the driver. Fig_2.2.4 shows the signs for drivers to stop the train. Therefore, the accuracy of stopping position is mainly based on the experience of the driver, which means it can not be absolutely ensured. Such misalignment will be from several to hundreds millimeters in practical condition.

Fig_2.2.4 Sign for stopping the trains [27]

As a summarize of chapter 2. Misalignment at hundreds millimeter occurs easily in railway WPT system and brings unreliable system performance.

Chapter 3--Configuration of Proposed System and a Method of Sensorless Coil Position Detection

To apply the proposed system into railway applications, several factors should be considered. For example, implementation of the system should save space for other devices, execution of position detection and control should be fast enough to save time for power charging, extra devices different from charging system should be avoided carefully to make the system simple. In this chapter, configuration of the whole system considering all these factors is introduced. Then specified design considerations for such system is discussed. Finally, detailed method is designed and verified by simulation results.

3.1 Configuration of proposed system
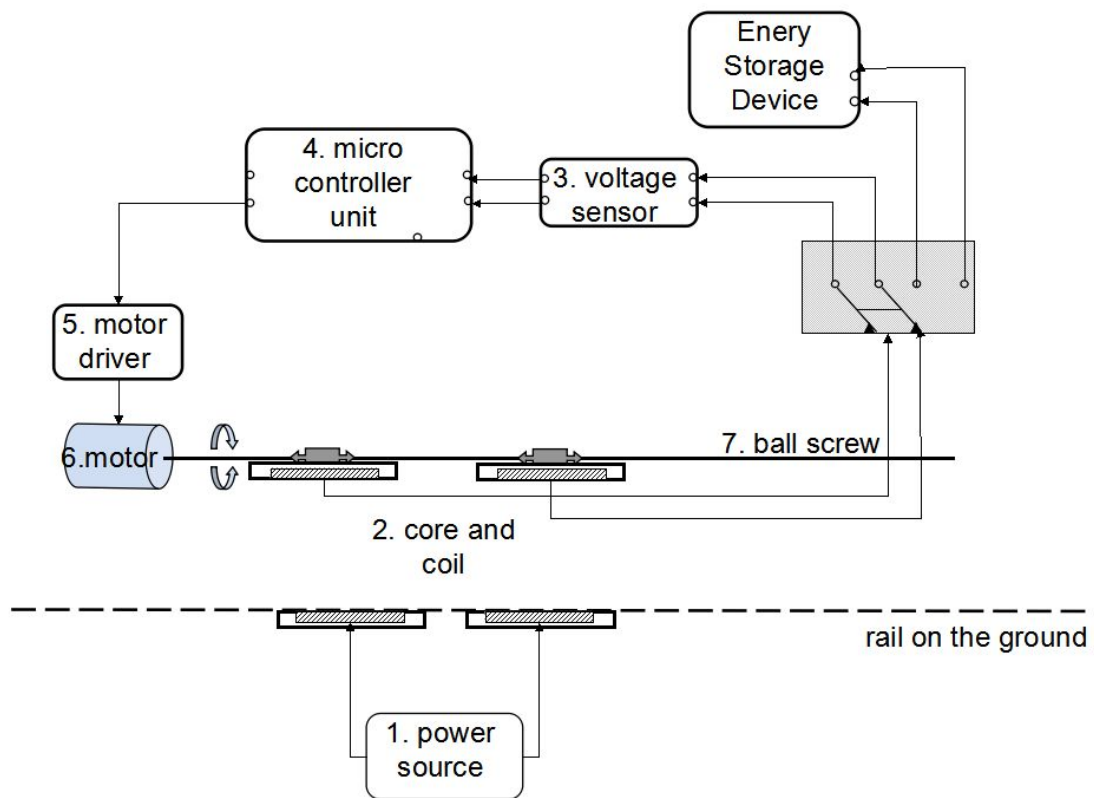
3.1.1 Configuration of proposed system

Moving coils to the aligned position is the basic idea of my proposed system, so it is necessary to determine the moving side at first. Analysis is made mainly by considering following factors:

(1) Form the viewpoint of economical, cost of actuators are calculated (appendix A). From this calculation, although the difference is not large, number of actuators will be less if they are implemented on trains.
(2) From the viewpoint of maintenance, actuators need to be checked and maintained more often than coils. In this system, primary side is buried underground and sealed closely to prevent affecting by rain or dust, and this brings difficulty to frequent maintenance.
(3) Form the viewpoint of emergency , only one train will be affected if error happens to an on-board actuator, but all the trains passing a station will be affected if error happens to an actuator implemented in station. As a consequence, actuators are choose to be implemented on the train. Thus, a simplified figure of system configuration can be drawn in Fig_3.1.1.

About the coils and cores. As described in chapter 2, the size of them should be confined within 800 mm. From the result of electromagnetic field analysis, interval between the coils at the same side should be larger than at least 1000 mm to avoid their interaction. In railway condition, average length of the vehicle is about 20 m,

thus the space is enough for implementing several coils. For the length of gap between primary and secondary coils, on one hand, it should be as short as possible to ensure high power transfer capacity and efficiency, on the other hand, enough gap length should be reserved to avoid coil collision. Thus here the gap is kept as 10 cm, and it shall be adjusted according to the specified conditions.

What's more, other devices such as voltage sensor and date processor (Micro Control Unit) are also needed to convert physical values to position information. All of them are included in the position detection system.

Fig_3.1.1 System configuration

3.1.2 Operation of proposed system
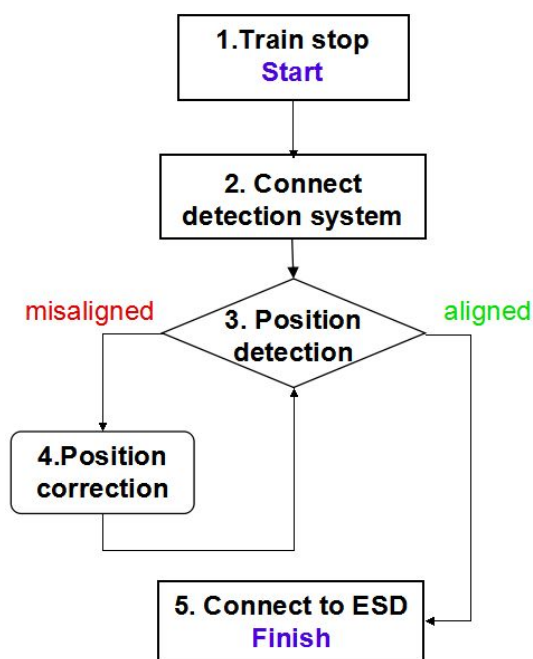
Fig_3.1.2 Operation sequence

Fig_3.1.2 shows the flow chart of operation sequence. At first, voltage sensor will be connected to replace the converter and ESD after the train stops. Power source at primary side will also be controlled at a much lower voltage to reduce power consumption of position detection. Then, position detection starts and position control will be executed if misalignment exists. Finally, after the coils are moved to the aligned position. Secondary coils will be reconnected to the converter and ESD again, also voltage at primary side will be increased for normal power transmission. Such sequence will be repeated at each station to keep the train always charged in the best condition.

3.2 Considerations of system design

General design considerations include requirements of detectable region, detection accuracy and system robustness.

I. Detectable region: It is the maximum misalignment which can be detected by proposed method. As mentioned in chapter 2, since it is much harder to control the stopping position of trains than EV, misalignment region can be from 0 to several hundred millimeters, at both front and rear direction. Therefore, the detectable should be designed as large as possible.

II. Detection accuracy: It is evaluated by comparing the error between actual and detected position. It dominates the performance of power charging. Inaccurate detection means the charging power will still be unstable and the

charging efficiency will still be low even position control is executed. From the analysis in chapter 2. To keep both power and efficiency deviation within 10%, misalignment of each coil should be controlled within 6.5% of coil length at the misalignment direction in this system.

III. System robustness: Though misalignment at left and right side seldom happen due to restriction of the track, deviation of gap length will happen due to many reasons such as differences in height between primary coils, distribution of passengers and lean of the vehicle body. For such reason, system robustness will be evaluated by the acceptable range of deviation.

3.3 Study of system coils characteristics

Since secondary coils are choose to be moved due to the discussion in 3.1.1, position signal should also be obtained form secondary side for a simple signal processing system. If position detection system and control system are at different sides, wireless signal transmission device will be necessity to transmit signals to secondary side. Therefore, system characteristics at secondary side are studied.

### 3.3.1 Relation between electromagnetic field and misalignment distance

In precedent research of Matsuoka [33], electromagnetic field characteristic is studied by using JMAG simulation. Fig_3.3.1 and Tab_3.3.1 shows the module and general parameters of the core. Fig_3.3.2 shows how inductance changes with the increasing of misalignment.
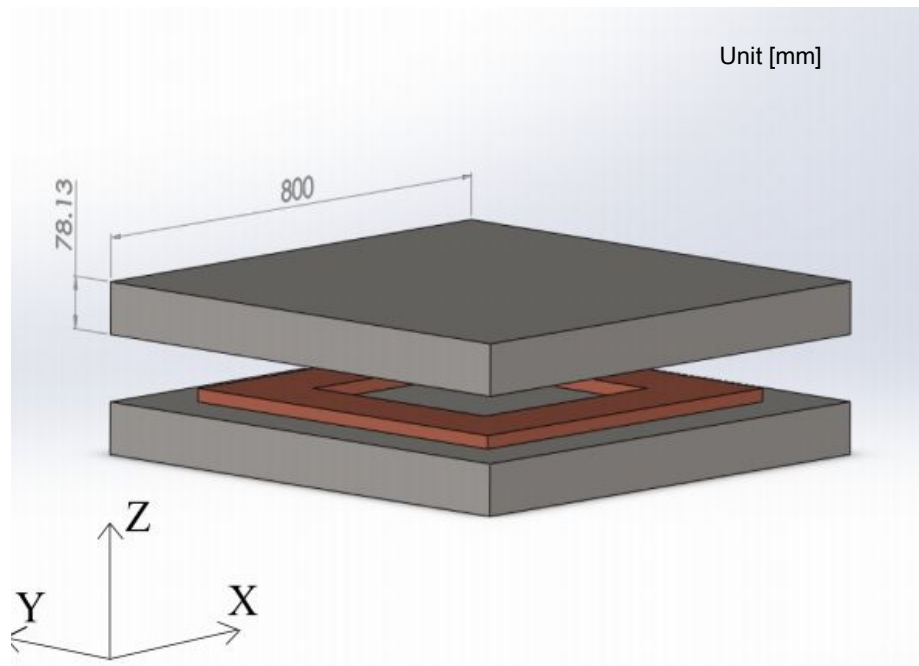
Fig_3.3.1 Module for analysis [33]

Tab_3.3.1 Parameters for analysis

| Parameter		Value	Unit
Core	length	800	mm
	width	800	mm
	height	78.13	mm
	material	ferrite	/
Coil	turns	20	/
	layers	5	/
	material	Φ 1.6 copper wire	mm
gap		100	mm
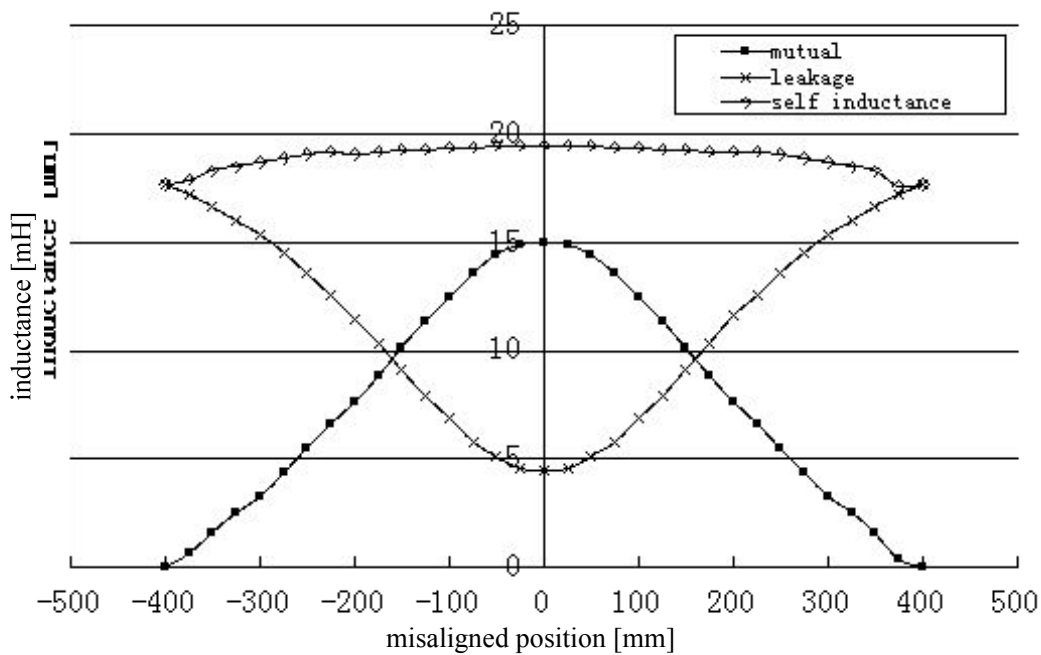
Fig_3.3.2 Inductance at difference misaligned position

From Fig_3.3.2, mutual inductance M increases and leakage inductance $L1$ decreases with the increasing of misalignment distance Dm. Value of self inductance Ls, sum of mutual inductance M and leakage inductance $L1$ decrease slower than mutual inductance. As the result, coupling coefficient k will decrease with increasing of misalignment.

3.3.2 Relation between electromagnetic field and gap length.

To analyze the influence of gap deviation on detection result, how electromagnetic field changes with gap length is studied. Fig_3.3.3~Fig_3.3.5 show comparison of inductance and coupling coefficient, in case of 10 cm gap and 8 cm, respectively.

When gap length is shorter, mutual inductance will be larger due to the closer magnetic coupling, however it drops faster with the increasing of misalignment. On the contrary, if the gap length becomes larger, mutual inductance will become smaller but drops slower with misalignment increasing. As a result, coupling coefficient as well as the induced voltage will be different in two cases.
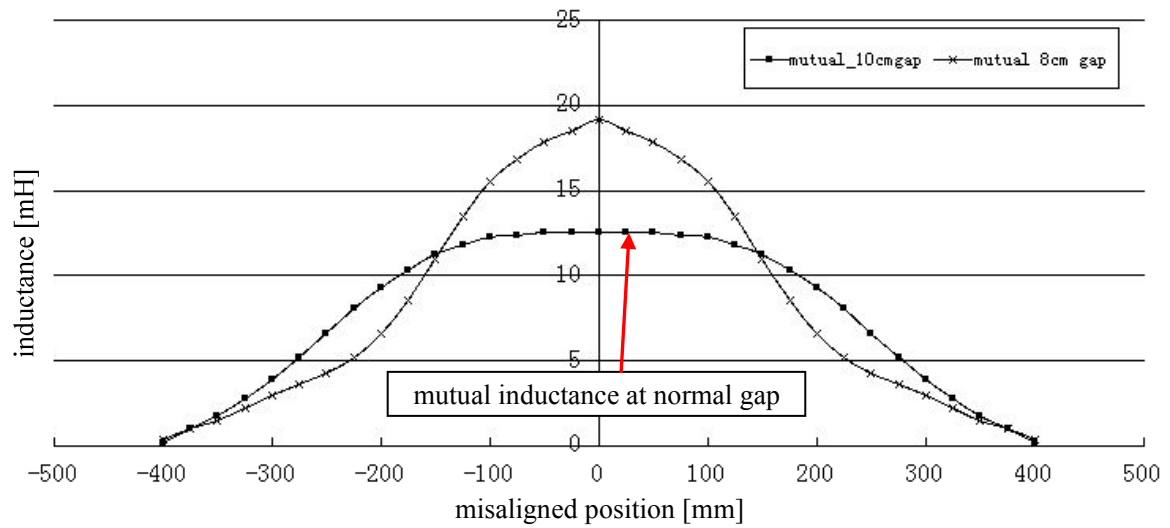

Fig_3.3.3 Mutual inductance
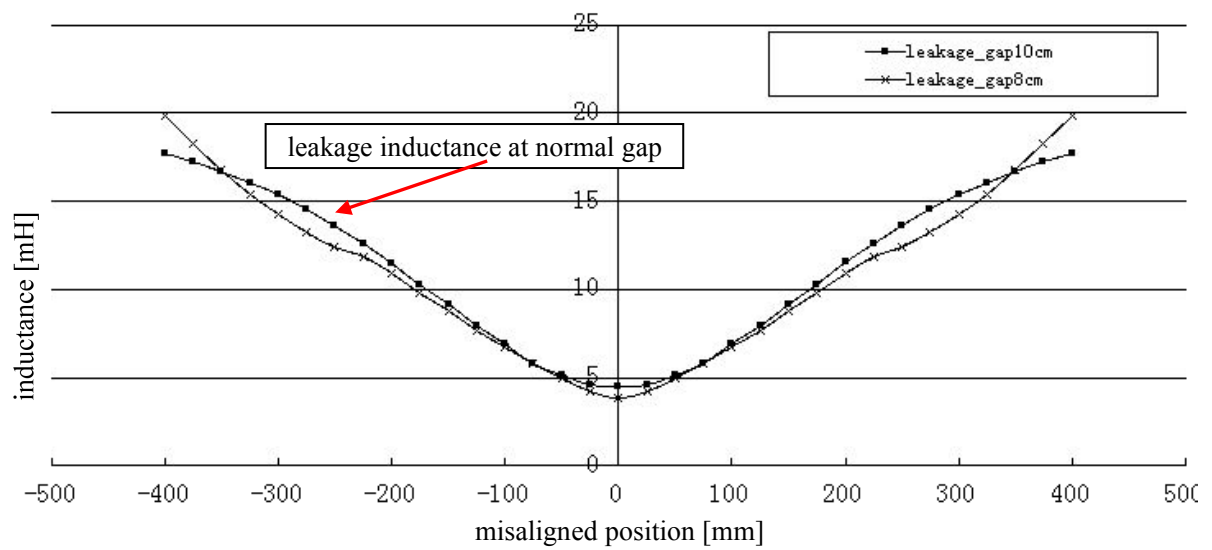
Fig_3.3.4 Leakage inductance
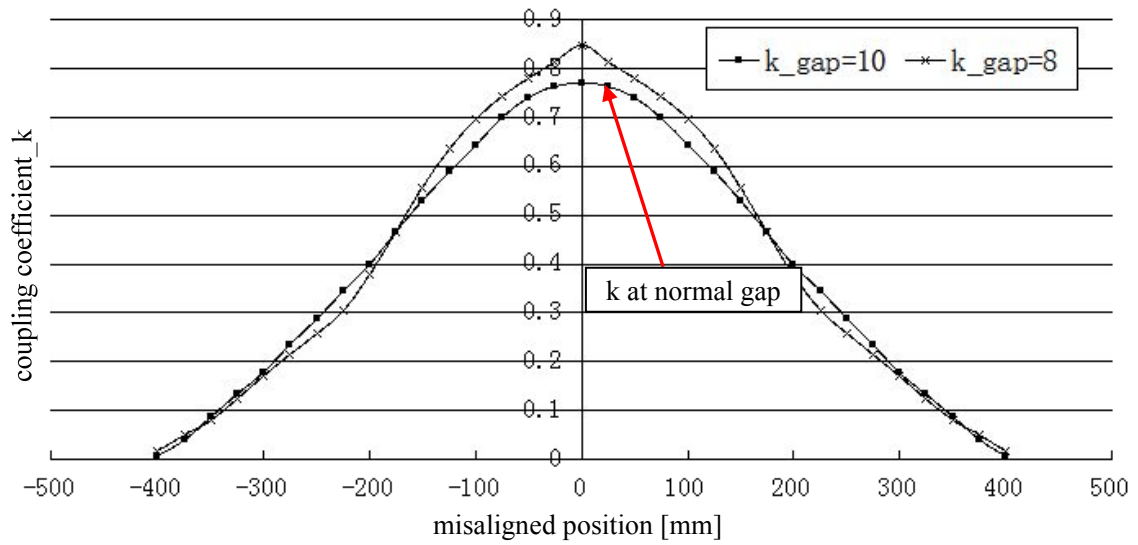
Fig_3.3.5 Coupling coefficient

3.3.3 Relation between electromagnetic field and induced voltage

Chapter 2 shows the characteristic of induced voltage over the load, but it is not suitable for stationary detection. So here if we increase the frequency of power source and make the secondary open-circuit, a new equivalent circuit can be drawn as Fig_3.3.6 (appendix B). Then relation between $V2$ and $V1$ can be obtained in eq.(3-1)~eq.(3-3)
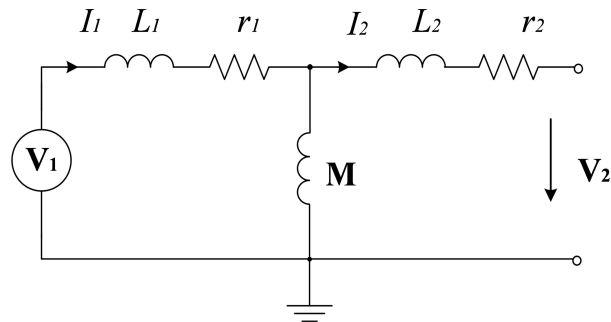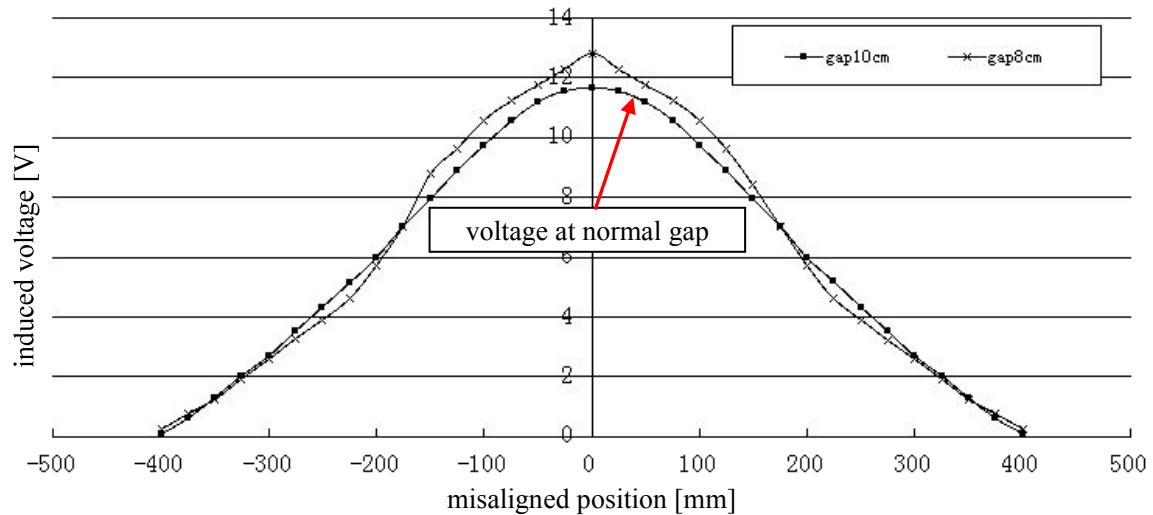

Fig_3.3.6 Equivalent circuit

$$V_1 = j\omega(M + L_1)I_1 + I_1 r_1 \qquad (3\text{-}1)$$

$$j\omega M I_1 = V_2 \qquad (3\text{-}2)$$

$$V_2 = \frac{j\omega M}{j\omega(M + L_1) + r_1} V_1 \qquad (3\text{-}3)$$

Form eq.(3-3), induced voltage is proportional to the distance of misalignment. Fig_3.3.7 shows its value when secondary side is at different misaligned position, while the gap length are 10 cm and 8 cm, respectively. Power source voltage is set to be $V1$=15 V, f=5 kHz.

Fig_3.3.7 Induced voltage at each misaligned position

This figure indicates that the amplitude of induced voltage can be used to express distance of misalignment monotonically, and this characteristic can be selected to detect the misaligned position in our system.

3.4 Details of system designing and simulation result

In this section, the author proposed methods to detect the direction and improve the robustness against gap deviation as well. All the basic data is obtained from the simulation module in section 3.3.1. Designed method is verified by simulation results.
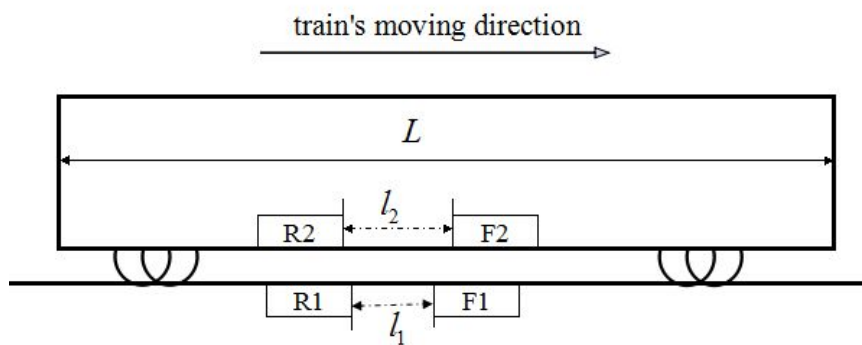
3.4.1 Direction detection

As described in chapter 2, this system will execute positioning after the train stops, which means static electromagnetic characteristic of coils should be used. From above analysis, amplitude of the induced voltage is proportional to the misalignment distance when secondary side is open-circuit. Basically, characteristic curve in Fig_3.3.7 can be used to make the positioning. However, there will be some problems if only one couple of coils is used for position detection. First of all, position of secondary coils can be either before or after primary coils along the moving direction of the train. Since this voltage-distance characteristic curve is symmetry, the induced voltage will be identical if the misalignment distance is symmetrical, which means the direction information can not be obtained by only using this curve. Also, gap deviations can happen between primary and secondary coils and change the gap

length, which brings errors if only the characteristic curve of a single couple of coil is used to calculate misalignment distance.

Therefore, a detection method using two-couple coils is proposed. This system includes a rear couple of coils R1&R2 and a front couple of coils F1&F2. They will be implemented with a certain spatial offset, from which the desired direction information can be obtained.

Fig_3.4.1 is a simplified figure which shows how the spatial offset is generated, $l1$ represents the interval between primary coils, $l2$ represents the interval between secondary coils and L is the length of the vehicle. To generate the spatial offset, $l2$ is set to be 50 mm larger than $l1$. Also, as explained in section 3.1, both $l1$ and $l2$ are set two be larger than 1 m to avoid the interference between coils form different couples. Center of primary coils is defined as the aligned position for secondary coils, and relation between misaligned distance of each secondary coil, R2 and F2, and the position of secondary coil center can be obtained in Tab_3.4.1.


Fig_3.4.1 Simple figure of arrangement of coils
Trains moving direction is defined as positive direction

Tab_3.4.1 Difference of distance at different misaligned position

R2&F2 center [mm]	-400	...	-50	-25	0	+25	+50	...	+400
R2 [mm]	425		75	50	25	0	25	...	375
F2 [mm]	375		25	0	25	50	75	...	425

From this table, when the center of secondary side is just above the center of primary side, misalignment distance of R2 and F2 will be the same. If secondary center is moved afterward, misalignment distance of R2 will always be larger. And on the contrary, misalignment distance of F2 will be larger if the center is moved forward. Such difference in distance will generate difference in induced voltage. Details are as follows.

When both primary coils R1 and F1 are connected to the same power source V1, the system can be expressed by using the equivalent circuit in Fig_3.4.2. And induced voltage at two secondary coils can be expressed in eq.(3-4) and eq.(3-5), resistor is ignored due to its small value when compared with inductor.
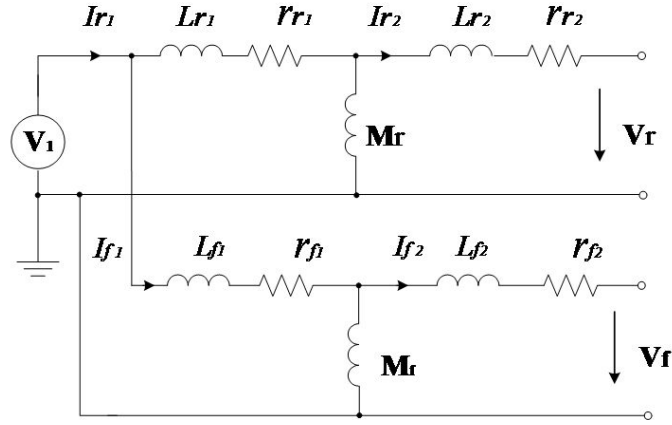
Fig_3.4.2 Equivalent circuit

$$\hat{V}_r = \frac{M_r}{L_{r2} + M_r}\hat{V}_1 \tag{3-4}$$

$$\hat{V}_f = \frac{M_f}{L_{f2} + M_f}\hat{V}_1 \tag{3-5}$$

From eq.(3-4) and eq.(3-5), voltage and phase of Vr and Vf are as same as that of $V1$. However, since there is difference of misalignment distance between these two couples of coils, amplitude of induced voltages will be different. So eq.(3-4) and eq.(3-5) can be changed to eq.(3-6) and eq.(3-7).
.

$$\hat{V}_f = V_f \cos(\omega t) \tag{3-6}$$

$$\hat{V}_r = V_r \cos(\omega t) \tag{3-7}$$

If power source is set as $V1$=15 V, f=5 kHz. Fig.8 can be drawn after calculating the amplitude of induced voltages when secondary side is at different misaligned position. Therefore, comparison of amplitude of induced voltage is applied to detect the direction, details are defined as follows:

(1) In region A ($Vf>Vr$), center of secondary coils is behind the aligned position, direction of secondary coils is defined as negative (-).
(2) In region B ($Vr>Vf$), center of secondary coils is before the aligned position, direction of secondary coils is defined as positive (+).
(3) At point C ($Vf=Vr$), center of secondary coils and the aligned position is overlapped, direction of secondary coils is defined as zero (0).

To achieve such comparison and generate the direction signal Va for signal processing system, process expressed from eq.(3-8) to eq.(3-9) is used.
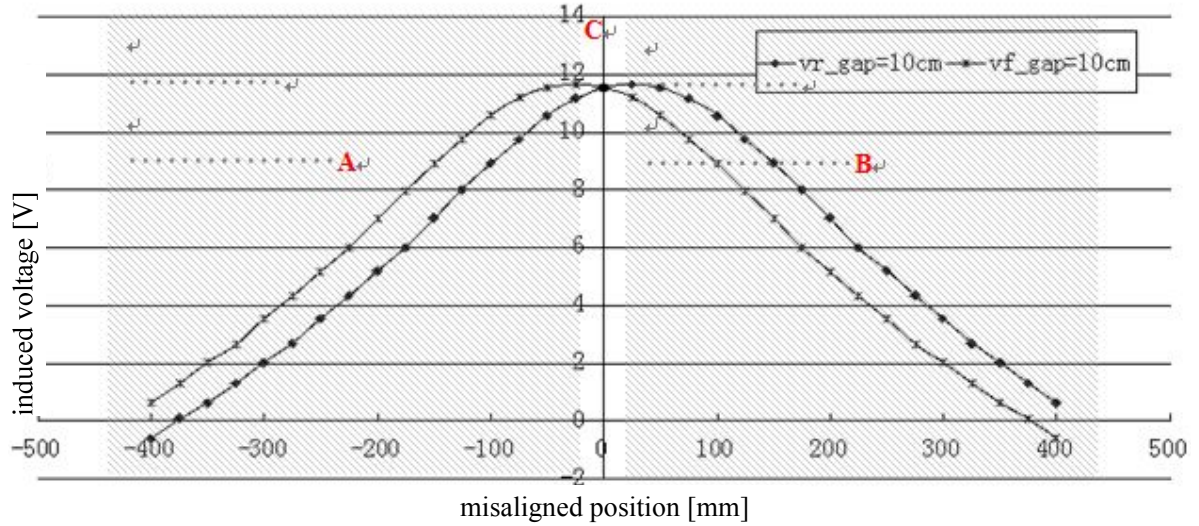
Fig_3.4.3 Different regions for comparing

$$\hat{V}_{com} = (\hat{V}_r + \hat{V}_f)(\hat{V}_r - \hat{V}_f)$$
$$= (V_r^2 - V_f^2)\cos^2(\omega t)$$
$$= (V_r^2 - V_f^2)\frac{(1 + \cos(2\omega t))}{2} \qquad (3\text{-}8)$$

$$V_a = \frac{(V_{r-oc}^2 - V_{f-oc}^2)}{2} \qquad (3\text{-}9)$$

Vcom includes a constant part and an alternating part at double frequency of the power source. After passing a low pass filter, the constant part *Va* is obtained. Positive *Va* indicates that center of secondary coils is before that of primary ones, while negative *Va* indicates the opposite condition

Then function *sign(Va)* shows the direction in a simple way. Here, positive, negative and zero position defined above can be represented by +1, -1 and 0 respectively, as in eq.(3-10).

$$sign(V_a) = \begin{cases} 1 & (V_a > 0) \\ 0 & (V_a = 0) \\ -1 & (V_a < 0) \end{cases} \qquad (3\text{-}10)$$

Fig_3.4.4 shows the simulation result of *Va* and s*ign(Va),* which means the proposed method can be used to detect the direction of misalignment within the range of (-400 mm , +400 mm).

Moreover, this figure shows that there will be no direction signal when misalignment distance is larger than 50% coil length due to nearly no voltage is induced. This is the main reason for restriction in detectable range in this system.
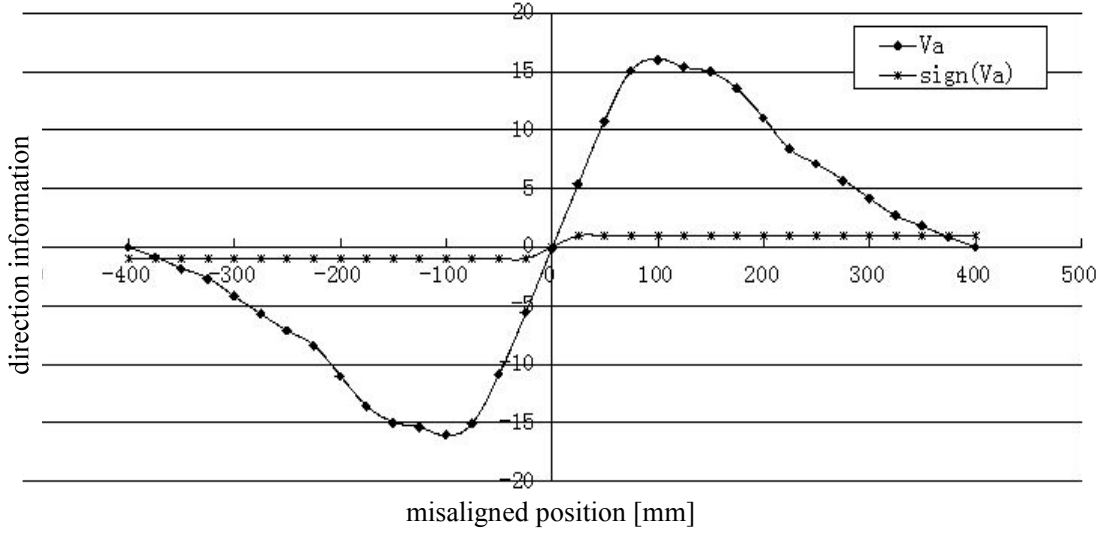
Fig_3.4.4 Direction signal at each misaligned position

3.4.2 Distance calculation

From discussion in section 3.3.3, amplitude of induced voltage is almost proportional to misaligned distance. So the basic idea is referring the detected voltage to such amplitude-distance characteristic to obtain the distance.

For the same reason in section 3.4.1, amplitude-position characteristic of a single couple of coils can not be directly applied to distance calculation. If gap deviation changes the gap length between coils, their coupling condition and the voltages induced will also be changed. Therefore errors will occur if the amplitude-distance characteristic curve obtained at the original gap length is still used to make distance calculation.

To reduce such error and increase robustness of detection system, voltages form two secondary coils are combined to obtain the distance, as shown in eq. (3-11)-(3-13).

$$
\begin{aligned}
\hat{V}_n &= \hat{V}_r \hat{V}_f \\
&= V_r V_f \cos^2(\omega t) \\
&= V_r V_f \frac{(1 + \cos(2\omega t))}{2}
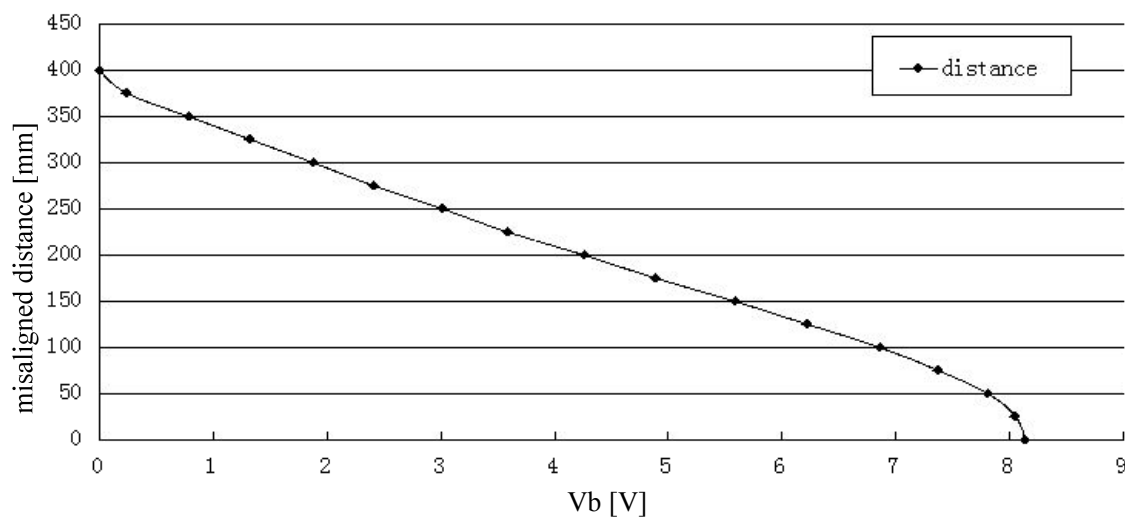\end{aligned}
\tag{3-11}
$$

$$
V_{nf} = \frac{1}{2} V_r V_f
\tag{3-12}
$$

$$
V_b = \sqrt{V_{nf}} = \sqrt{\frac{1}{2} V_r V_f}
\tag{3-13}
$$

Vn is the product of *Vr* and *Vf*. Also, after passing a low pass filter, only the constant part *Vnf* is left. *Vb* is the root of *Vnf*, its value at different position is shown in Fig_3.4.5. This curve can be transferred into a distance-amplitude characteristic curve, as in Fig_3.4.6 Finally, by combing calculated *Vb* and this distance-amplitude characteristic characteristic curve, misalignment distance *Dm* can be calculated.
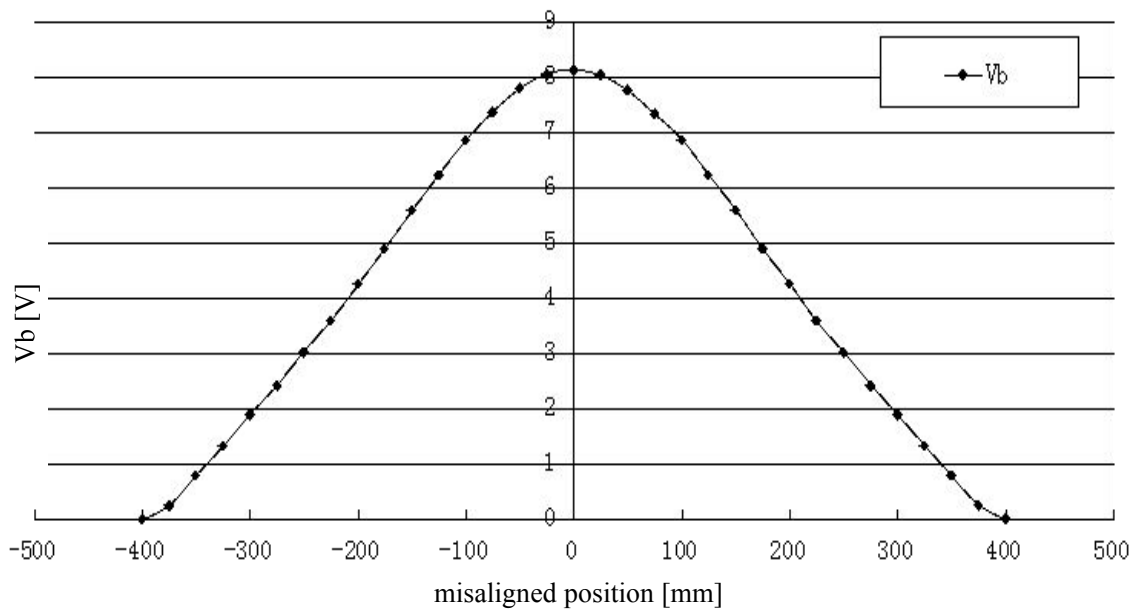

Fig_3.4.5 Vb for distance calculation

Fig_3.4.6 Distance-voltage characteristic curve

After both *sign(Va)* and *Dm* are obtained, finally detected misaligned position Pm can be calculated in eq.(3-14). Simulation is made to detect the misaligned position of secondary coils, when they are put at each misaligned position and the result is shown in Fig_3.4.7. From this result, the proposed system can be used to detect coil

misalignment within the range of (-400 mm , 400 mm), about 1/2 coil length at each direction accurately.

$$P_m = D_m \cdot sign(V_a) \qquad (3\text{-}14)$$
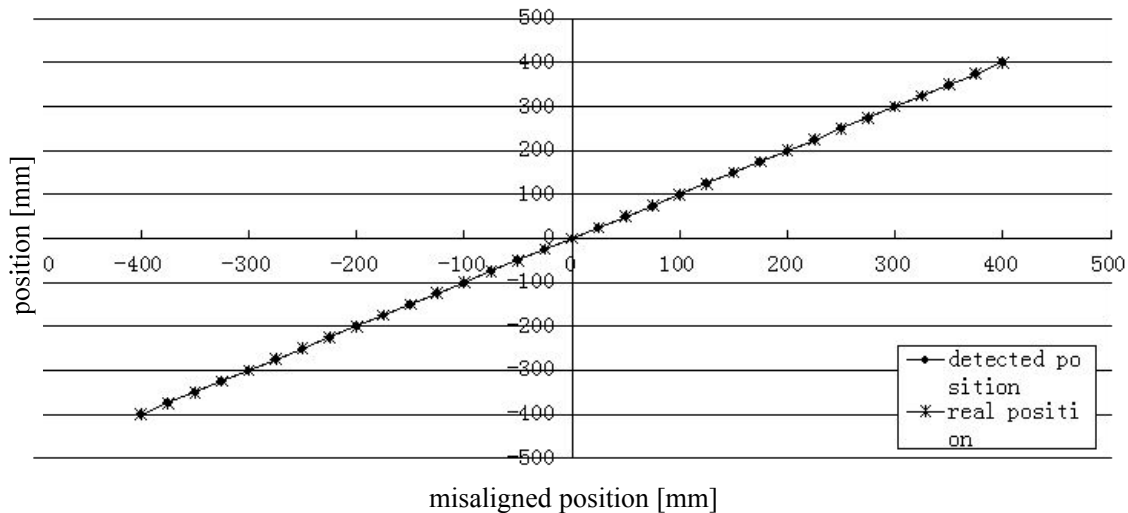
Fig_3.4.7 Detected position at each misaligned position

3.4.3 Affects of gap deviation

Form section 3.3.2, gap deviation will bring changes to inductance value, as well as effect the induced voltage. Error analysis of detected position information are made in two cases. Details are as follows:
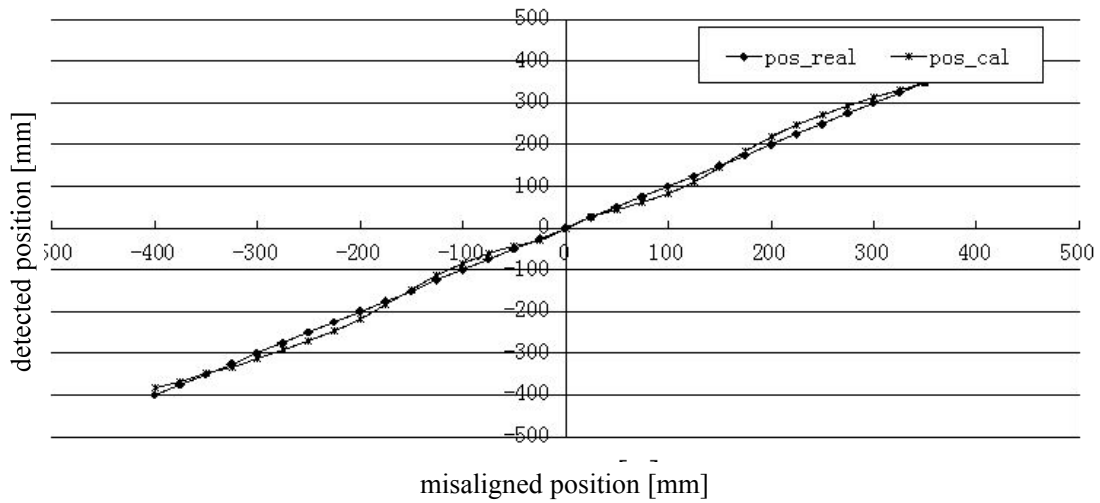
Case 1: R1&R2 gap=8 cm, F1&F2 gap=8 cm.

In this case, both gap between R1&R2 and F1&F2 are reduced by 20% from the original one. Thus the induced voltage in R2 and F2 will be the same, and both will increase due to the decrease of gap length, as shown in Fig_3.4.8. Fig_3.4.9 shows comparison of the detected position and real position, and Fig_3.4.10 shows the error between them.

From such result, if the gap deviations are the same. Only the detected distance will change. In this case, maximum error of detected position is about 23 mm, so the maximum error for a signal coil is 48 mm after considering spatial offset, about 6% of the core length. Detection of aligned position is still correct, which means the final position after control will still be right.
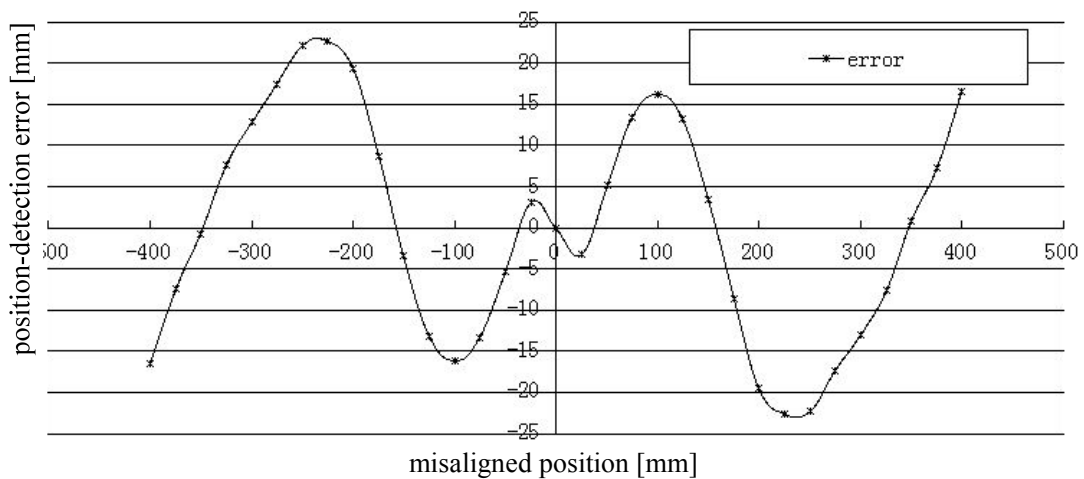
However, this situation is not an usual one. Usually, gap deviation will make difference in gap length, and position detection in such situation will be discussed in case 2.
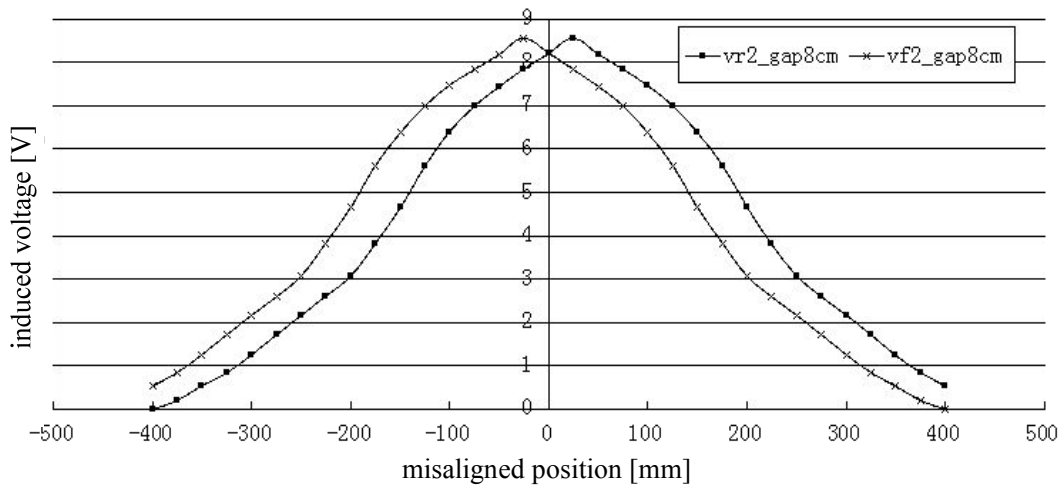
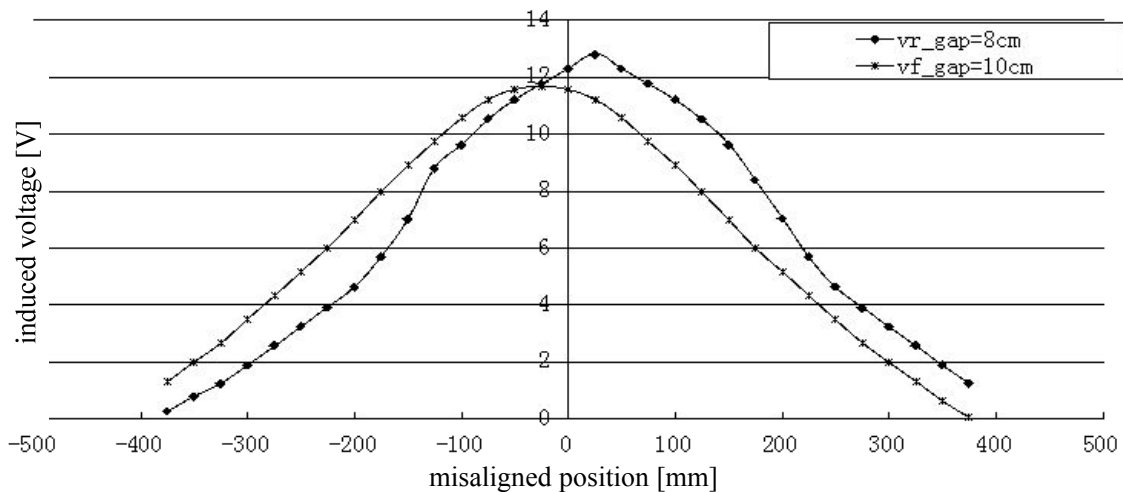Fig_3.4.8 Induced voltage at each misaligned position

Fig_3.4.9 Detected position at each misaligned position

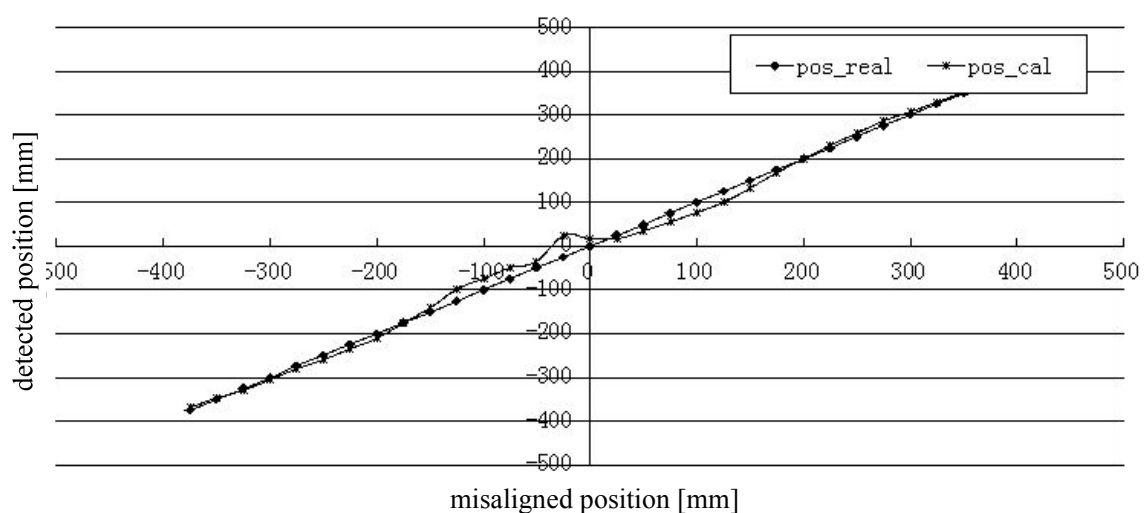Fig_3.4.10 Error in position detection at each misaligned position

Case 2: R1&R2 gap=8 cm, F1&F2 gap=10 cm

This case shows a more often situation: gap changed in different length. In this simulation, R1&R2 gap is reduced by 20%, while F1&F2 gap stays unchanged.
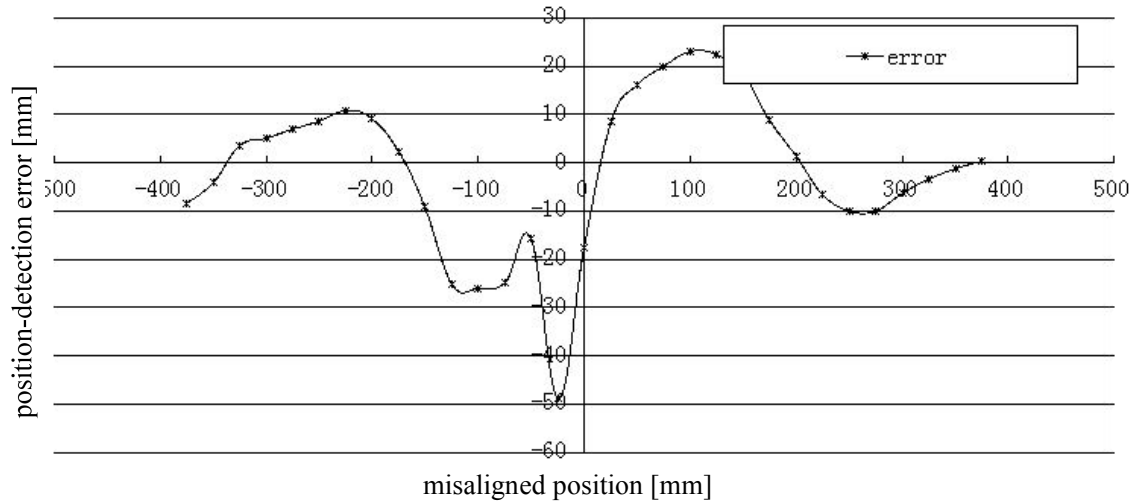

Fig_3.4.11 Induced voltage at each misaligned position

Fig_3.4.11 Fig_3.4.12 and Fig_3.4.13 show the induced voltage, detected position and errors, respectively. From this result, if gap length are different, both detected distance and detection information will be affected. Detected aligned position will move to the side where the induced voltage is smaller. When misaligned position of secondary side is about -25 mm, detected direction is wrong and thus the biggest error occurs. This error is about 50 mm, so misaligned position for a signal coil will be 75 mm after considering the spatial offset, which means a failure in positioning.

Fig_3.4.12 Detected position at each misaligned position

Fig_3.4.13 Error in position detection at each misaligned position

3.4.5 Method to eliminate gap deviation affect

By observing the curve in Fig 3.4, detection error is mainly caused by the changed maximum amplitude of induced voltage. If such change in maximum induced voltage can be eliminated, detection errors will be eliminated as well. To achieve such objective, a method which uses curve normalizing is proposed. If dividing amplitude of the induced voltage at each misaligned position by their maximum value, a new normalized voltage-position characteristic curve can be obtained. The equation is as eq.(3-15), and normalized curve is shown in Fig_3.4.14

$$V_2^* = \frac{V_2}{Max[V_2]} \qquad (3-15)$$
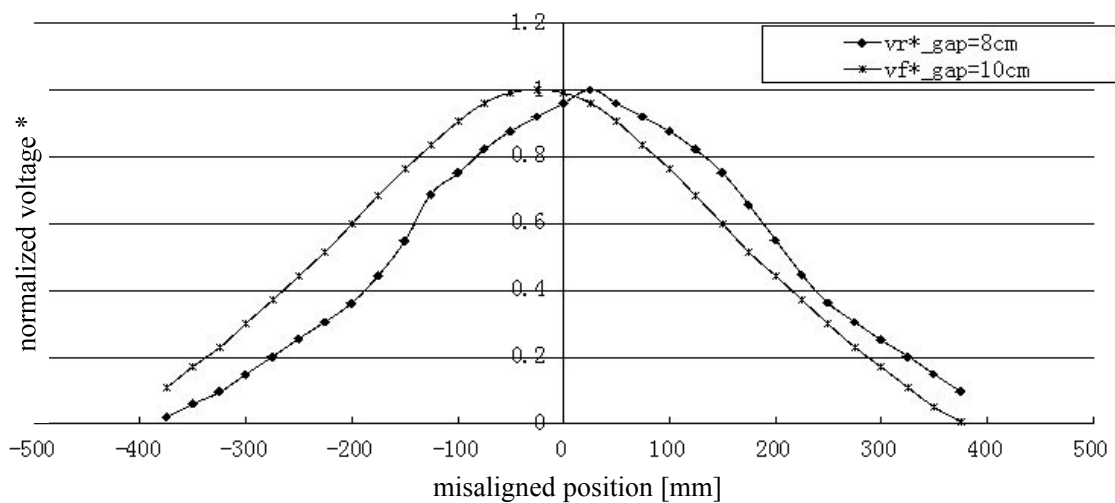
Fig_3.4.14 Normalized voltage-position characteristic curve

From this figure, difference of induced voltage caused by gap deviation are reduced. The detected aligned position is pulled back to the real aligned position again, which means the robustness of positioning is improved.

3.4.6 Sequence of position control

Position control will be executed after coil position is obtained. From the above analysis, the proposed method is able to detect the correct position with tolerance to gap length change, but the maximum amplitude of the detected voltage should be obtained. However, since the execution of positioning starts after train stops, the maximum value is unknown at the first. This means the a scanning is needed to obtain the maximum value of the voltages. Thus the execution can be divided into three phases:

Phase.I. Accessing relatively aligned position (close loop)
Purpose of this step is to reduced the scanning range. According to the above analysis, scanning is needed to obtain the maximum amplitude of the value of induced voltage. However, extremely large range is necessity to ensure the necessity data can be obtained if scanning is executed as the first, due to the lacking the initial position, especially direction information. On the other hand, though the position detected by original amplitude-position characteristic curve is inaccurate, it is not totally wrong, either. Misaligned position can be limited to a smaller range based on the original curve, thus the inaccurate aligned position can be regarded as an "approximately aligned" position in this system. By starting from this relatively aligned position, scanning range will be reduced.

Phase.II. Scanning (open loop)
Scanning will be started after coil stops at the approximately aligned position, in this system, scanning is set fixed based on the maximum error. Thus the maximum value can be obtained in all situations.

Phase III. Accessing accurate aligned position (close loop)
Finally, coil position will be controlled by using the normalized curve. Detected position will be used as feedback and compared with the position reference (0 mm). After the coil reaches aligned position, operation is finished.

Chapter 4--Experimental Verification

Chapter 4 shows the experimental verification of proposed position detection and control method. First of all, experiment objective, which is based on design objective, is shown in section 4.1. Selection and implementation of hardware is discussed and shown in 4.2. Finally, experiment process is shown and results are discussed in section 4.3 and 4.4.

4.1 Experiment objective

Accuracy and robustness of designed method are main factors to be verified in this experiment.

Accuracy is evaluated by comparing the estimated position and actual position. From the design objective discussed in chapter 2, maximum acceptable misalignment for each coil after position control should be less than 50 mm. Since a smaller scale experiment set (will be explained in section 4.2) is selected in this experiment, acceptable misalignment for each coil in should also be 1/5 of the real one, so it is 10 mm. Considering the spatial offset between two couple of coils, the maximum acceptable misalignment of secondary side center is 5 mm.

Robustness is evaluated by comparing the accuracy when gap deviation happens in different cases. And this will be assessed by the acceptable range of gap deviation, when requirement accuracy can be ensured.

Therefore, objective of this experiment is as follows

(1) Verify if the designed system can detect and control coil position accurately within 5 mm.

**(2) Make assessment of system robustness against gap deviation.**

4.2 Selection and implementation of hardware

4.2.1 Cores and coils

In real application, ferrite cores and coils at the scale of 800*800 mm are used for transmission of high power (100 kW) . Since this experiment is built to verified the position detection method but not the power transfer ability, and position of coils are detected based on the shape of inductance-position characteristic curve of the coil. Smaller scale equipment set can be selected if it can be used to verified the proposed position detection method.

In this experiment, as shown in Fig_4.2.1, the equipment at 1:5 ratio of the real size are used. Gap length is also reduced at the same ratio to remain the ratio at vertical direction [34].

Coil turns number is kept as the same as the real one. Turns of coils are selected as 20 (turns) x 5 (layers). Wires are ϕ 1.6 copper wire, which are used in usual WPT applications. Parameters of the core and coils are as shown in Tab_4.2.1.
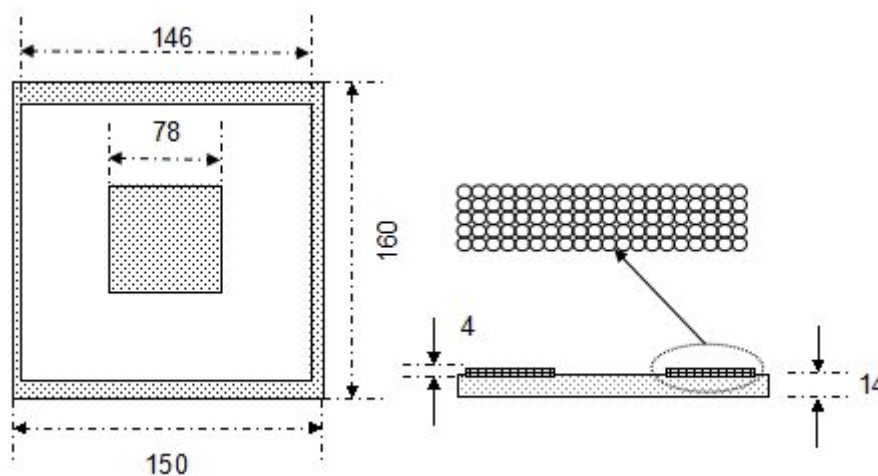
Fig_4.2.1 Core and coils--unit [mm]

Tab_4.2.1 parameters of core&coil

Parameter		Value	Unit
Core	length	160	mm
	width	150	mm
	height	10	mm
	material	ferrite	/
Coil	turns	20	/
	layers	5	/
	material	Φ 1.6 copper wire	mm
gap		20	mm

Induced voltages at secondary side are measured to confirm their characteristic, as shown in Fig_4.2.2, here gap length is 20 mm. Form this figure, shape of voltage-position characteristic curve obtained from smaller core is similar to the one obtained from 800*800 mm core in Fig_3.3.7, thus the feasibility of smaller scale experiment set is verified.

4.2.2 Moving devices

For coils position control, linear actuator is needed to move the coils at horizontal direction linearly. Linear motor can be used to move stuffs in a line, however, interference between the magnetic fields of coil and linear motor will bring inaccuracy of position detection and control. Thus it is better to use transfer belt or ball screw, which has no magnetic field at moving part, to convert the movement of rotation motor to linear direction. In this experiment, ball screw is selected.

Length of core is 160 mm, detectable range is about (-80 mm, +80 mm). According to this range, 300 mm length ball screw is selected, as shown in appendix C.
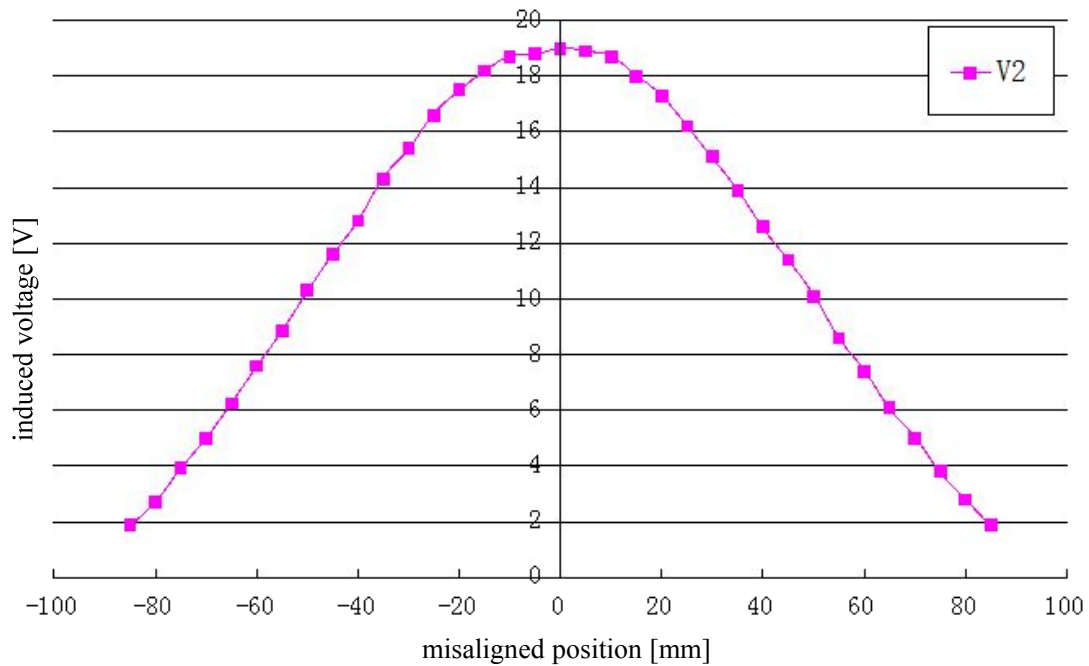
Fig_4.2.2 Induced voltage of 1:5 size core&coil

4.2.3 Implementation of hardware

Finally, the system is implemented as shown in appendix B. Generally, the primary side should be put on the ground, while in this system, considering the convenience of changing gap length and installing of actuator, the primary side is suspended above secondary side. Since the objective is to verified the performance of position detection and control, this way of implementation brings no influence to experiment results.

4.3 Position detection and control without considering gap deviation

In this section, performance of coil position detection and control without considering gap deviation (without scanning) will be evaluated by experiment. Two cases are studied, case 1 is the ideal condition, in which no gap deviation happens, while case 2 is an common condition, in which coil gap length are changed by deviation.

Case 1: R1&R2 gap=20 mm, F1&F2 gap=20 mm.
(1) position detection

Firstly, both gap length are set as 20 mm. Fig_4.3.1 shows the situation when misaligned position is -80 mm as an example. Power source at primary side is set as $V1=40$ V, $f=5$ kHz.
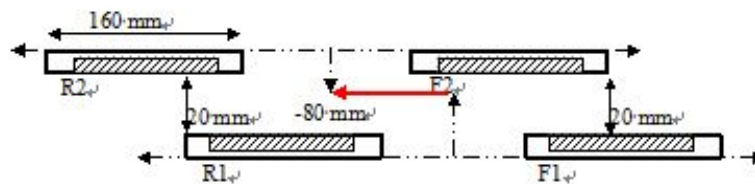

Fig_4.3.1 Coil arrangement at -80mm misaligned position

Amplitude of induced voltages at each misaligned position are measured, as in Fig_4.3.2. From this figure, amplitude-position character curve of Vr induced in coil R2 and and Vf induced in F2 are similar to each other, except some small difference caused by difference between each coil.
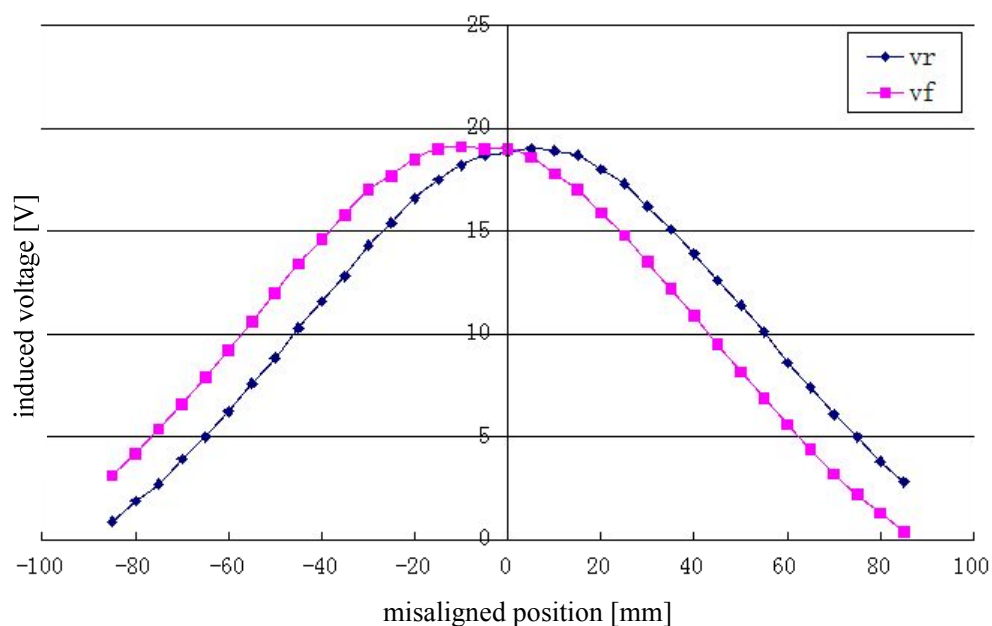
Fig_4.3.2 Induced voltage at 20&20 mm gap

Fig_4.3.3 shows the calculated position when secondary side is set at each misaligned position. And it can be seen form this figure that the position can be detected accurately. From this figure and analysis in chapter 3, controlling of coil position based on this curve are supposed to be accurate.
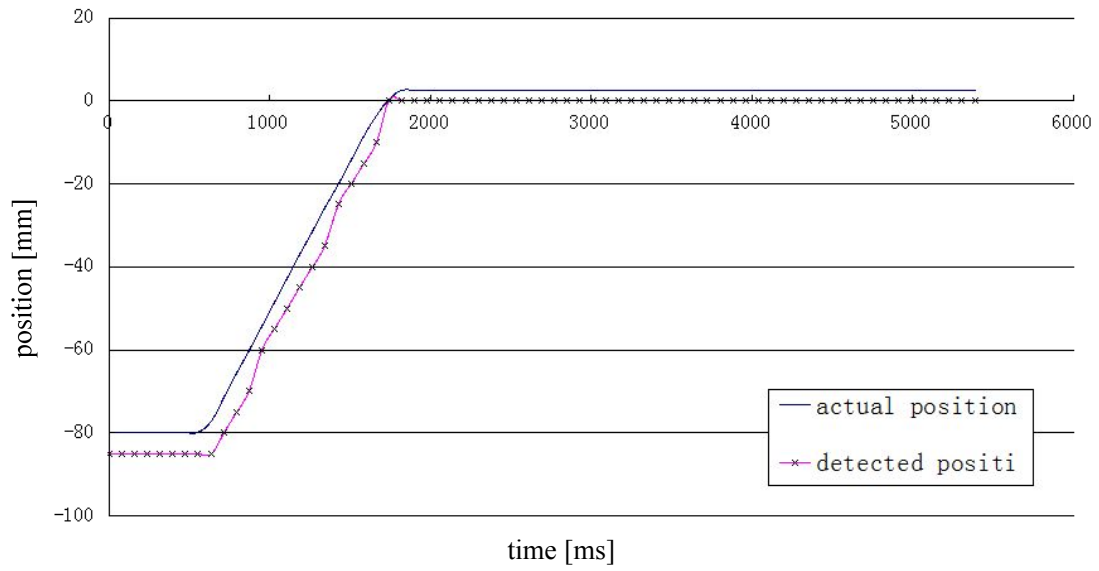

misaligned position [mm]
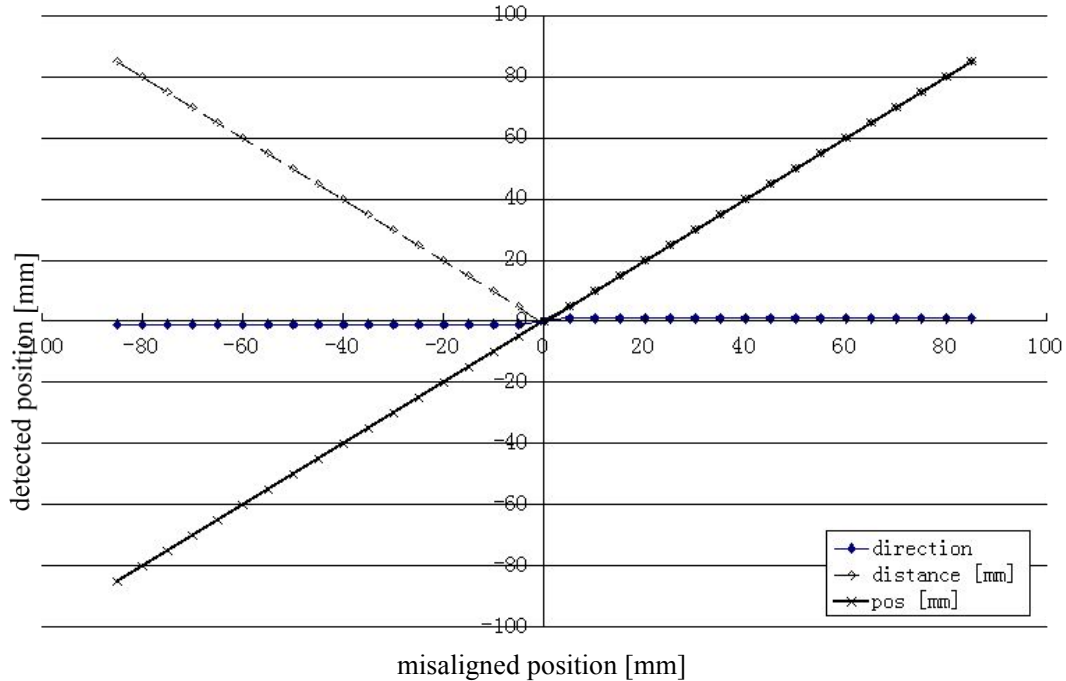
Fig_4.3.3 Position detected at each misaligned position

(2) Position control

Position control are executed form different starting points. Tab_4.3.1 evaluated the performance by the ending position after control and execution time. Fig_4.3.6 and Fig_4.3.7 show detailed performance when secondary side stops at -80 mm, the most rear condition, and 80 mm, the most front condition, respectively. Maximum execution time is less tan 2 s, 6.67% of dwelling time, if the average dwelling time is 30 s.

Tab_4.3.1 Performance in several cases

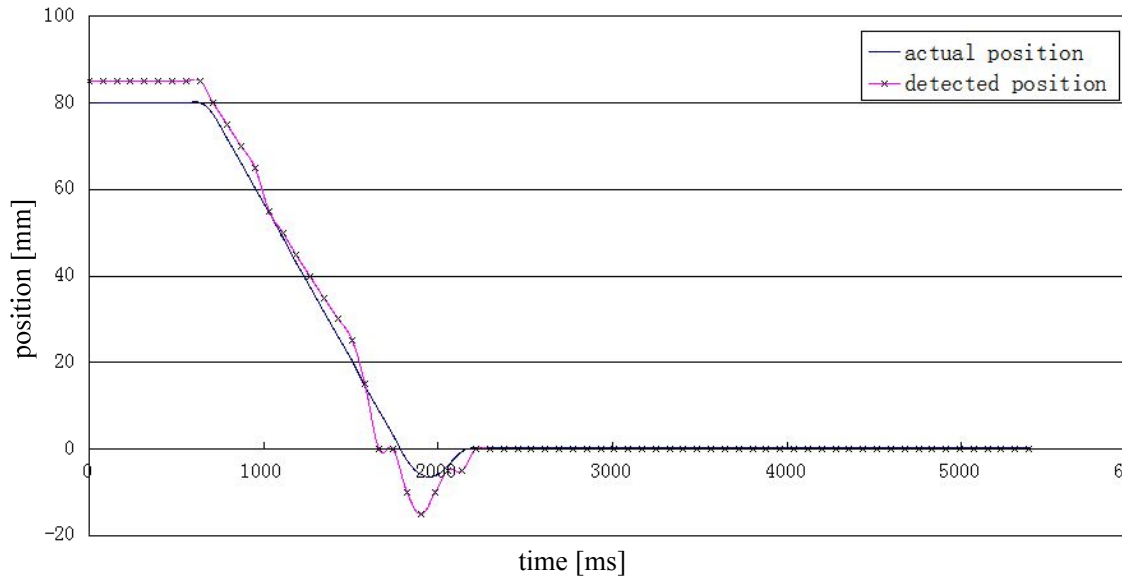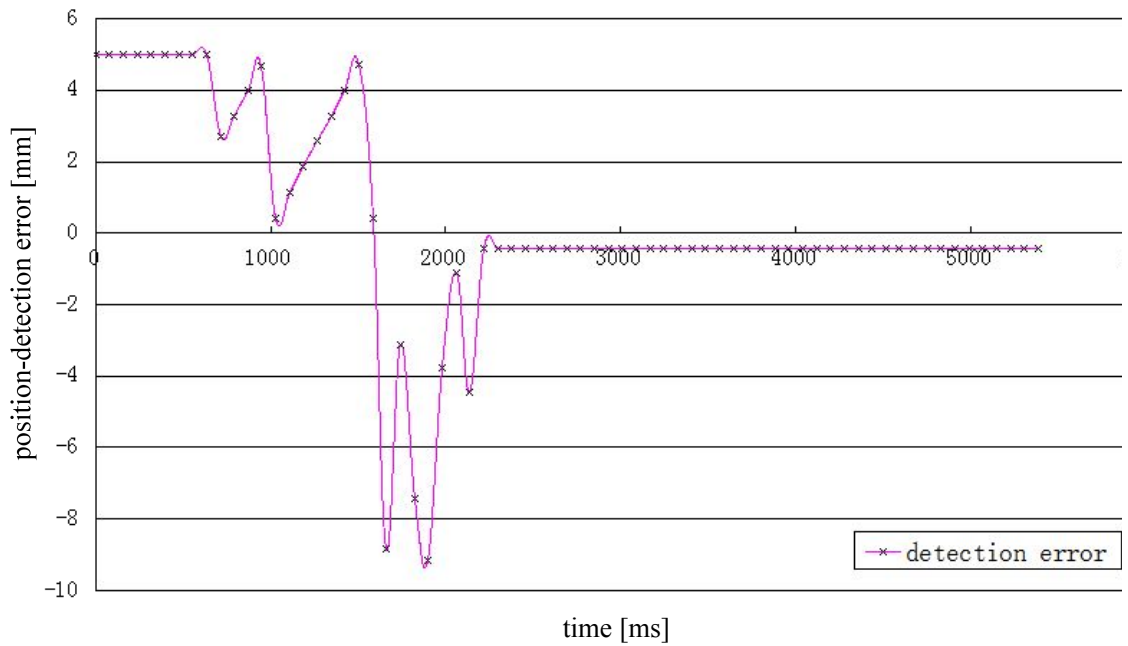| Case No.	Start position[mm]	End position[mm]	Time [s]
1	-80	-2.23	1.27
2	-50	-0.89	0.79
3	-20	-1.36	0.40
4	20	-1.1	0.71
5	50	-2.40	1.11
6	80	-1.73	1.58

(a)
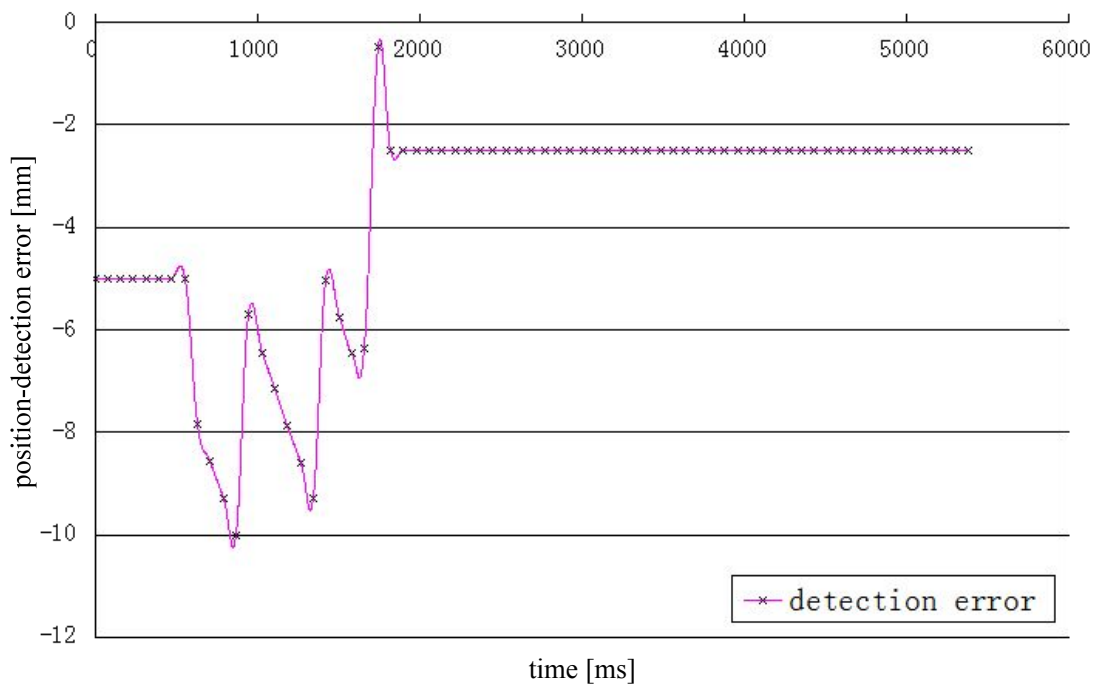
(b)

Fig_4.3.4 System performance without considering gap deviation--starts from
-80mm
(a) detected and actual position (b) detection error

Move to inaccurate aligned position based on original voltage-position characteristic
curve (close-loop)

(a)

(b)

Fig_4.3.5 System performance without considering gap deviation--starts from +80mm

(a) detected and actual position (b) detection error

Move to inaccurate aligned position based on original voltage-position characteristic curve (close-loop)

These result verified that the position can be controlled accurately when no gap deviation happens. The error of finally corrected position is less than 2.5 mm, which is smaller than 5 mm mentioned in experiment objective. Thus the accuracy of such system without gap deviation is verified.

**Case 2: R1&R2 gap=20 mm, F1&F2 gap=10 mm.**

This case studies the system performance with decreasing gap length. For instance, setting of coils at +50 mm misaligned position is shown in Fig_4.3.6. Power source at primary side is still set as $V1$=40 V, f=5 kHz.
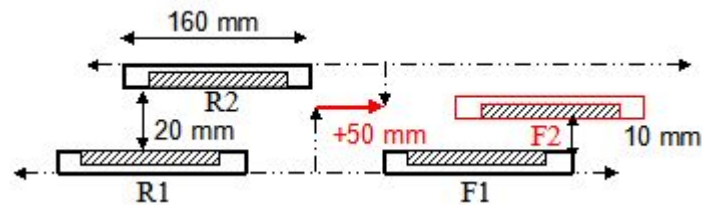

Fig_4.3.6 Arrangement of coils at +50 misaligned position

1) Position detection

Induced voltage and the calculated position are shown in Fig_4.3.7 and Fig_4.3.8, respectively. Unlike the curve in Fig_4.3.2, it is easy to notice the difference between induced voltages in two secondary coils in this curve. Since gap of R1&R2 is much larger than gap of F1&F2, amplitude of Vr is much smaller. In Fig_4.3.8 the aligned position, which is obtained by comparing amplitude of two voltage, are moved forward by about 40 mm, 25% of the coil length. Which means huge errors of position occurs due to such gap deviation. Also from Fig_4.3.8, direction signal becomes useless due to its low value, thus detectable range in this condition is (-80 mm, +80 mm) .
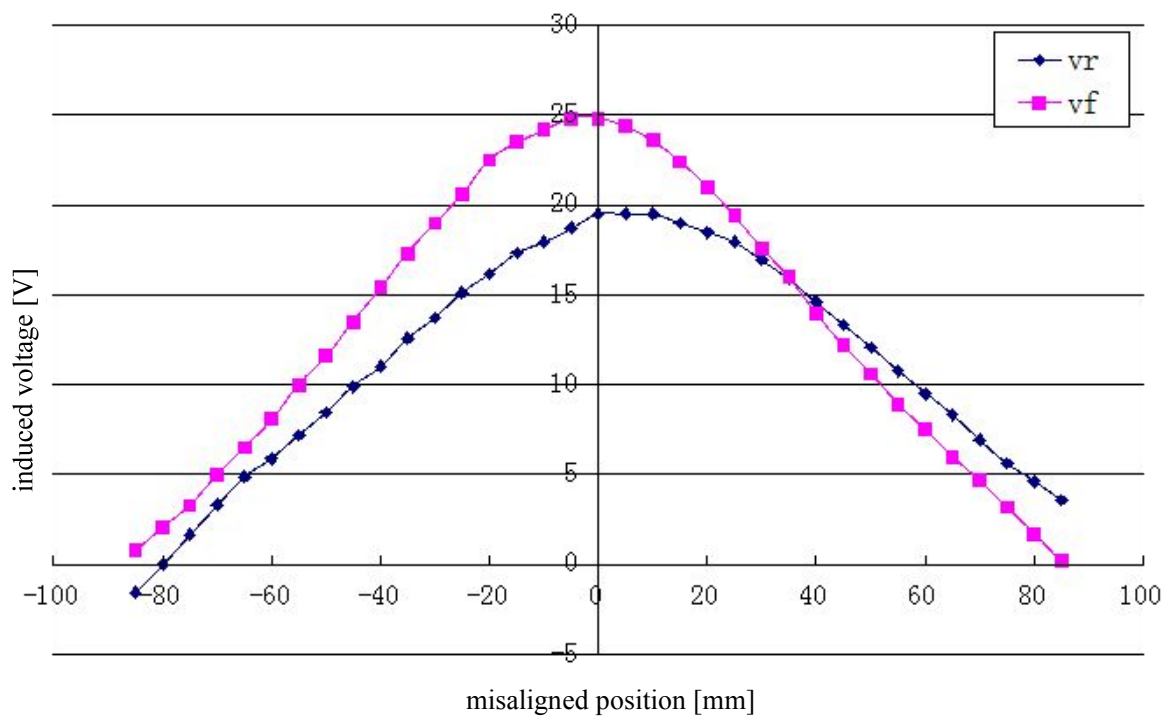

Fig_4.3.7 Induced voltage

misaligned position [mm]
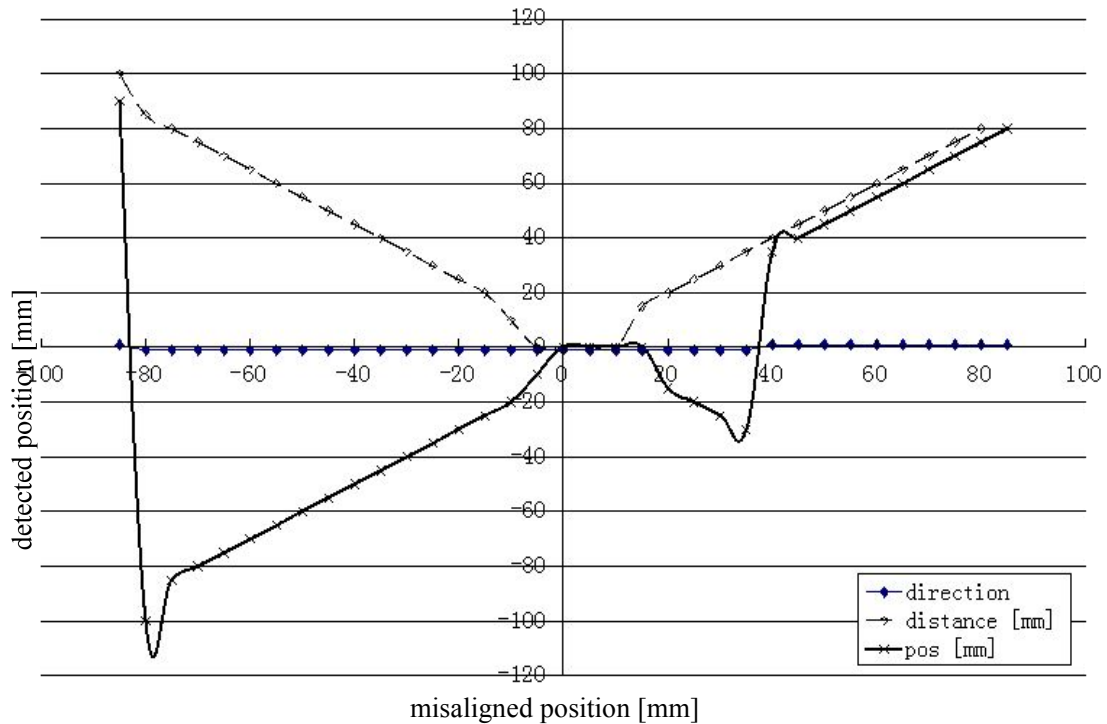
Fig_4.3.8 Position detected by using original curve at each misaligned position

At first, position will be just controlled directly based on this unnormalized amplitude-position characteristic curve to evaluate the error. Here the starting position is selected at +80 misaligned position. Result is shown in Fig_4.3.9. Here the actuator are stopped at a inaccurate aligned position due to the inaccurate position detection. Final position of secondary coils is at about +50 mm misalignment, which means that this position control is not successful. Several tests at other position are made and have the similar result. As a conclusion, gap deviation must be considered to make this system reliable.

time [ms]
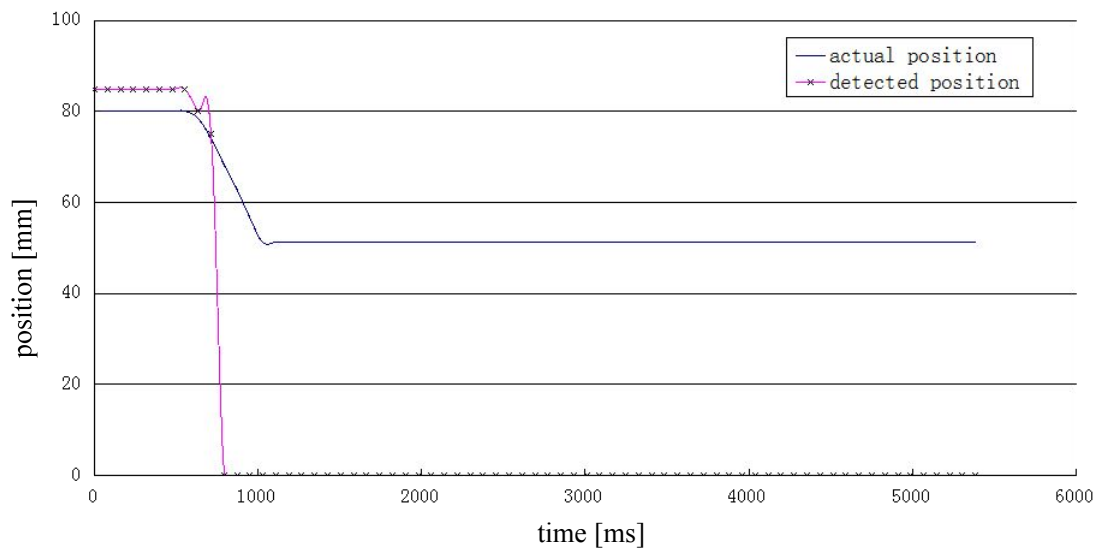
Fig_4.3.9 Position control based on original curve

4.4 Position detection and control with scanning for compensating gap deviation

The system performance was tested at different gap length to verify the robustness of the designed system in this section. And the situation of gap deviation are set as following:

Case 1: R1&R2=20 mm, F1&F2=10 mm

As discussed in the last section, position control at gap deviation will be unreliable, thus the proposed curve normalization are used in this section to improve system robustness. Coil setting in this case 1 is the same as the case 2 in the last section, for an obvious observation and comparison.
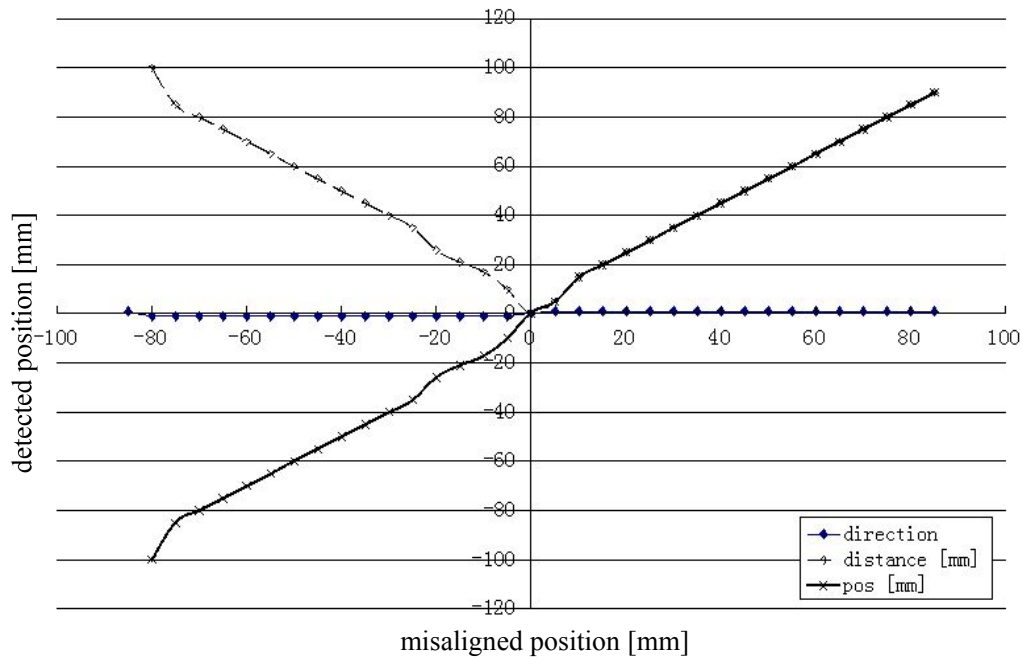
1) Position detection

Amplitude-position characteristic curve and position detected based on this curve are the same as Fig_4.3.1 and Fig_4.3.2, due to the same coil setting.

Now, the proposed curve normalization method is used to verify if it can be used to improve performance of position detection&control. Normalized curve is in Fig_4.4.1, detected position is in Fig_4.4.2.

misaligned position [mm]
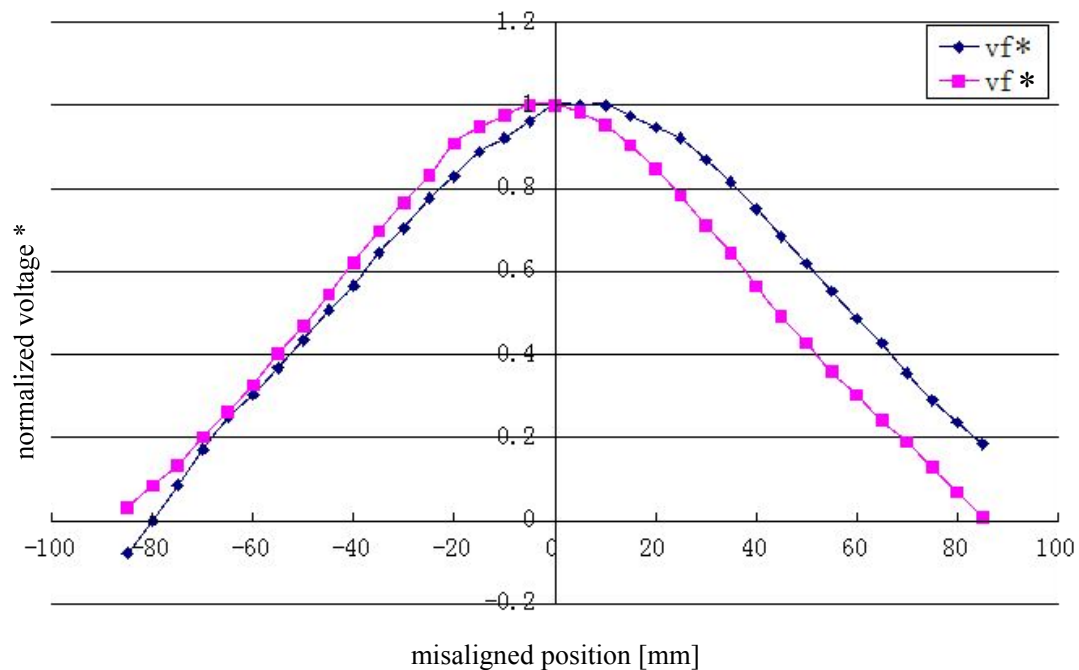
Fig_4.4.1 Normalized amplitude-position characteristic curve

From Fig_4.4.2, by using normalized curve, aligned position is detected correctly. Error in distance calculation still exists but are reduced substantially. Since the final objective is to move the coils to aligned position, errors at such scale in distance are supposed to be accepted.

Fig_4.4.2 Position detected by using normalized curve at each misaligned position

2) Position control

Operation sequence in this part is changed because scanning is used to improve system performance. Coils are moved to the approximately aligned position by using original curve at first, and then moved again to the accurate aligned position after scanning. Fig_4.4.3 and Fig_4.4.4 show the details of system performance when secondary coils are at -80 mm and 80 mm, the most rear and most front position.

From Fig_4.3.1, aligned position before curve normalization is at +40 mm. When the secondary side reaches this position, detected position will be 0 mm and thus scanning will be started. Difference between position calculated form original and normalized curve can be easily observed form Fig_4.4.3 and Fig_4.4.4. Firstly, aligned position is corrected from +40 mm to 0 mm, which means the direction information is detected accurately. Secondly, the maximum distance error is reduced, form about 15 mm to less than 5mm in the end. As the consequence, the performance of position control can satisfy the experiment objective, correct coils position within the range of -5 mm~+5 mm, with the gap changed by -50% of original length, in this case.
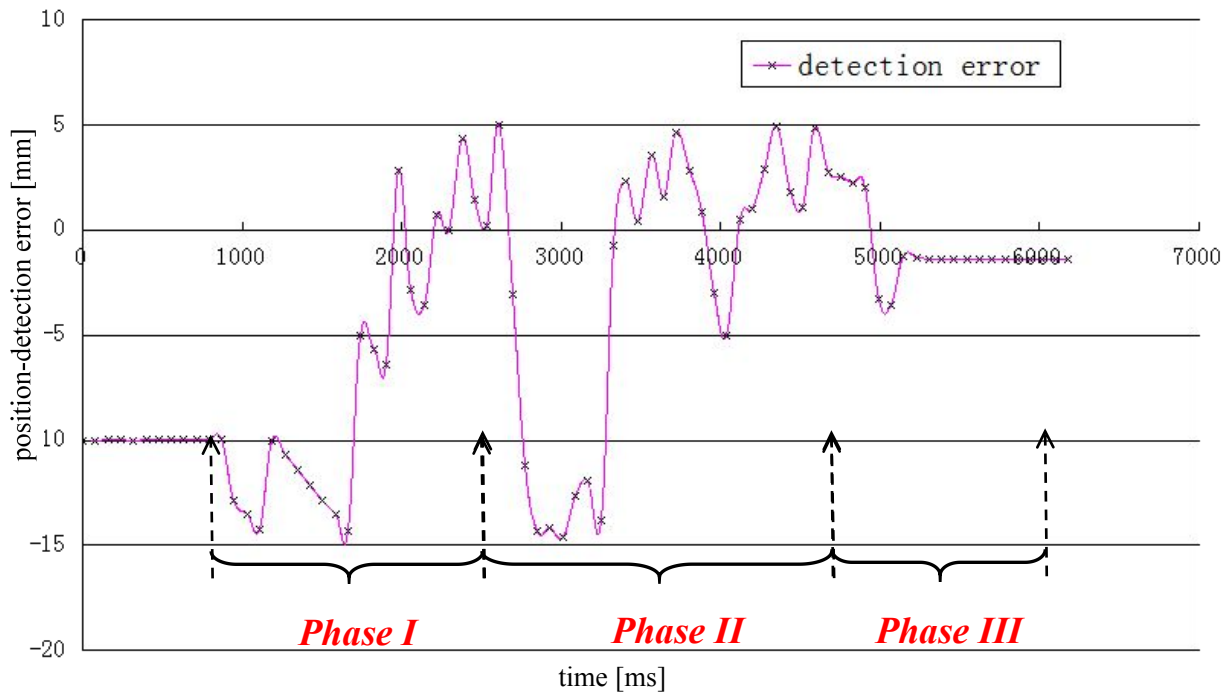
Position control performance in several other cases are observed, results are shown in Tab_4.4.1. These results also verified the robustness of designed system.

Tab_4.4.1 Performance at each starting position

| Case No	Start position[mm]	End position[mm]	Time [s]
1	-80	-2.51	4.36
2	-50	-0.10	3.96
3	-20	-0.30	3.56
4	20	-0.76	2.97
5	50	1.26	3.33
6	80	1.34	3.80
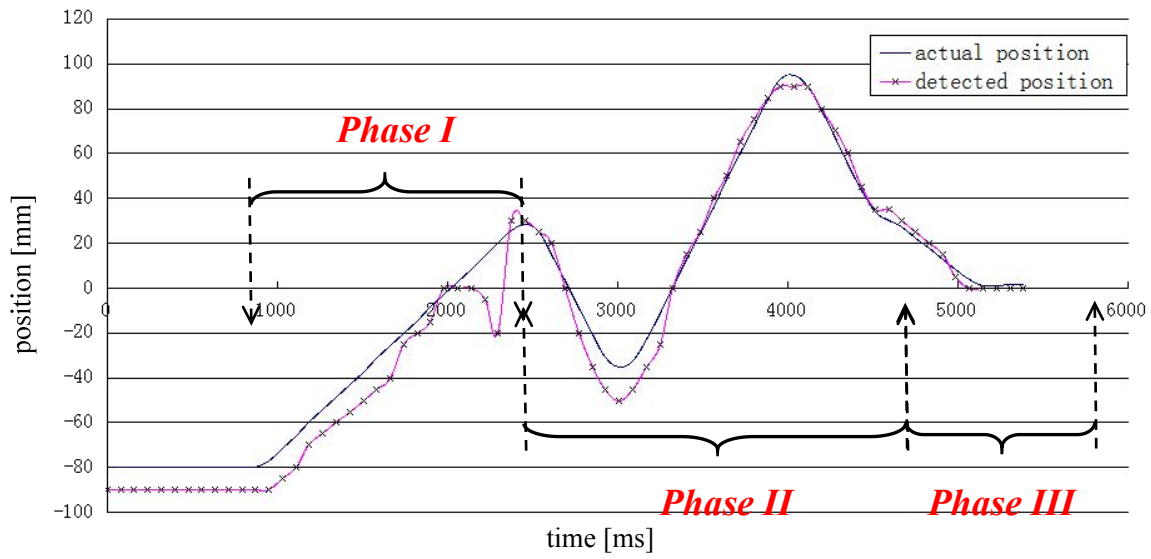
(a)

(b)

Fig_4.4.3 System performance--starts from -80 mm
(a)detected and actual position (b) detection error

Phase I: Move to inaccurate aligned position based on original voltage-position characteristic curve (close-loop)
Phase II: Scanning with fixed distance (open-loop)
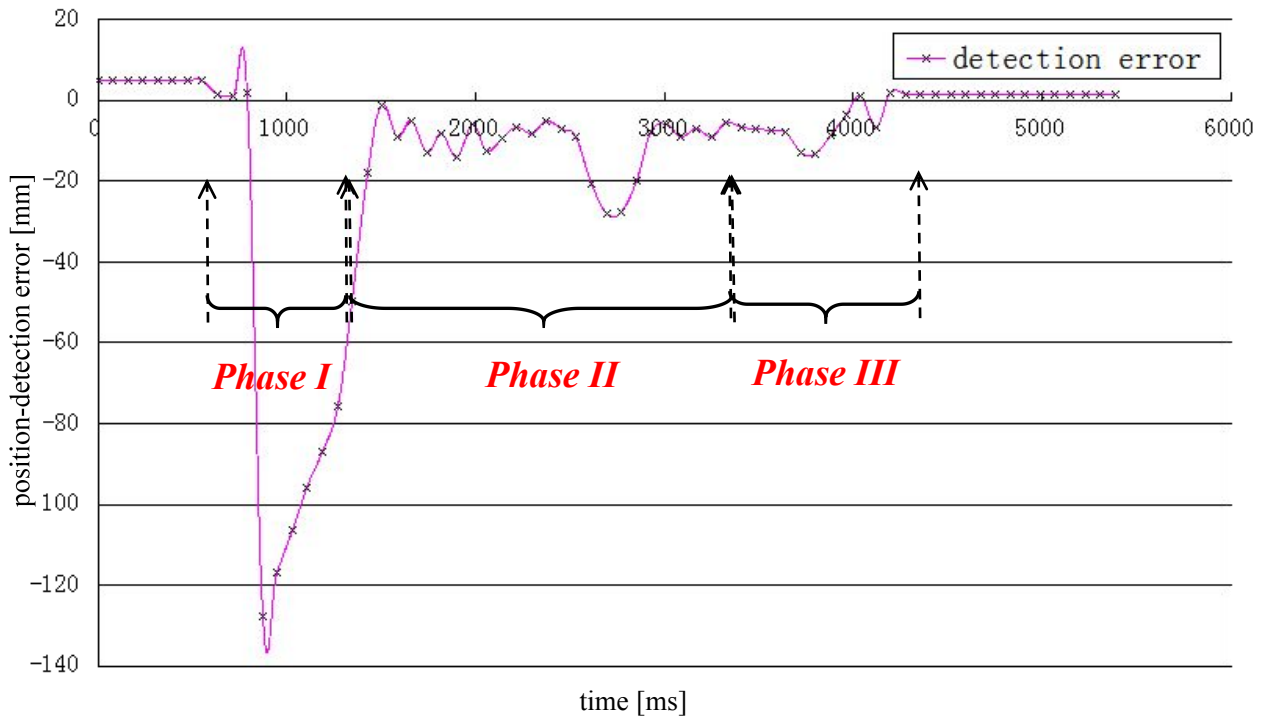Phase III: Move to accurate aligned position based on normalized curve(close-loop
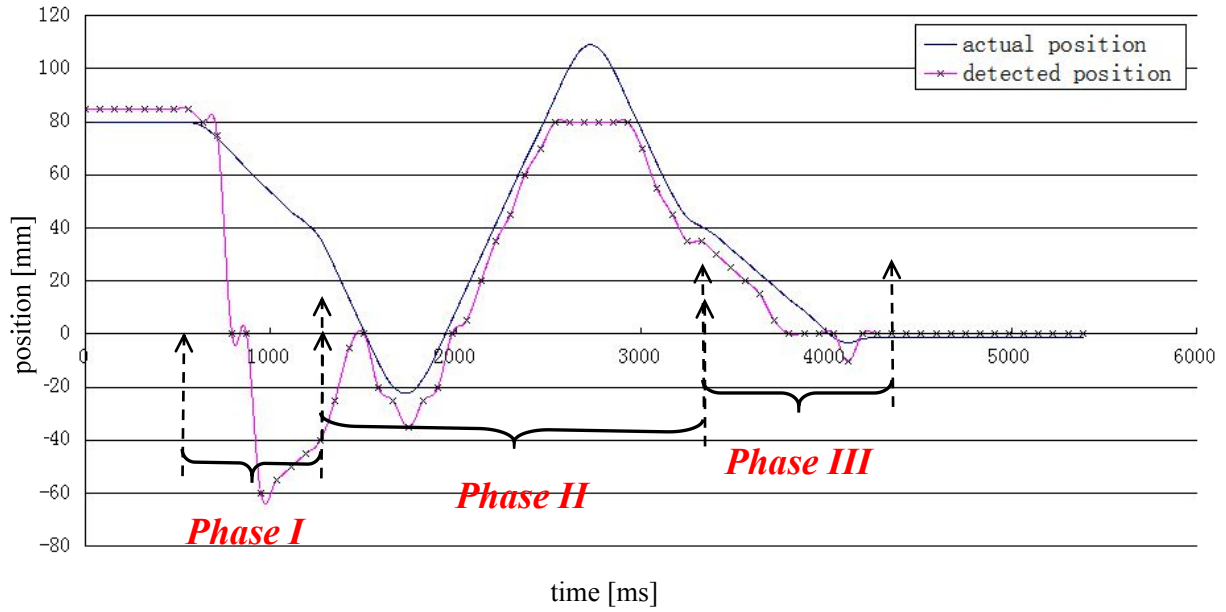
(a)

(b)

Fig_4.4.4 System performance--starts from +80 mm
(a) detected and actual position (b) detection error

Phase I: Move to inaccurate aligned position based on original voltage-position characteristic
curve (close-loop)
Phase II: Scanning with fixed distance (open-loop)
Phase III: Move to accurate aligned position based on normalized curve(close-loop

Case 2: R1&R2=20 mm, F1&F2=40 mm

This case studies the system performance with increased gap length, as shown in Fig_4.4.5. Induced voltage is shown in Fig_4.4.6. In the case, gap of R1&R2 is less than gap of F1&F2, so the *Vr* induced in R2 is larger than the *Vf* induced in F2. Because of this, the detected aligned position is moved -50 mm from the accurate one, which still leads to huge error in positioning. Moreover, calculated distance is increased due to the increasing of average gap length, as shown in Fig_4.4.7. Both of them lead to inaccurate in position detection.
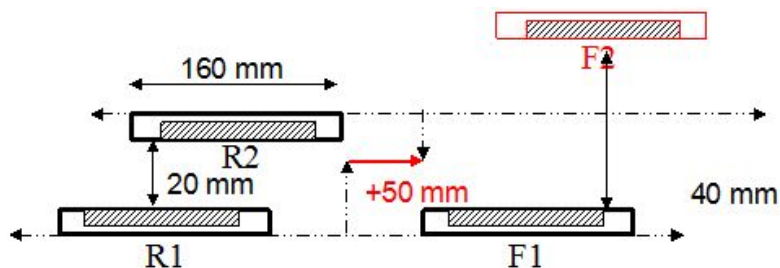

Fig_4.4.5 Gap setting at +50 mm misaligned position
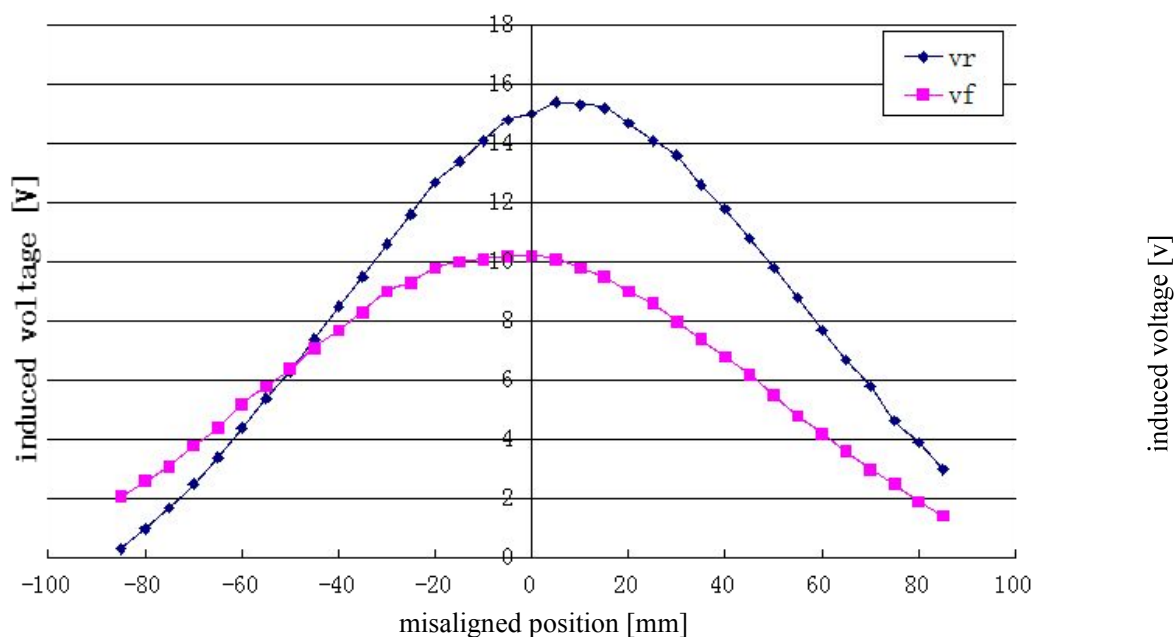
Fig_4.4.6 Induced voltage in R2 and F2

Then the normalized curve are used to eliminate the errors caused by gap deviation, as in Fig_4.4.8 and Fig_4.4.9. Results indicate that errors of aligned position are restricted within 5 mm, and maximum error of distance detection is reduced to 5 mm, both of which are in the acceptable range.
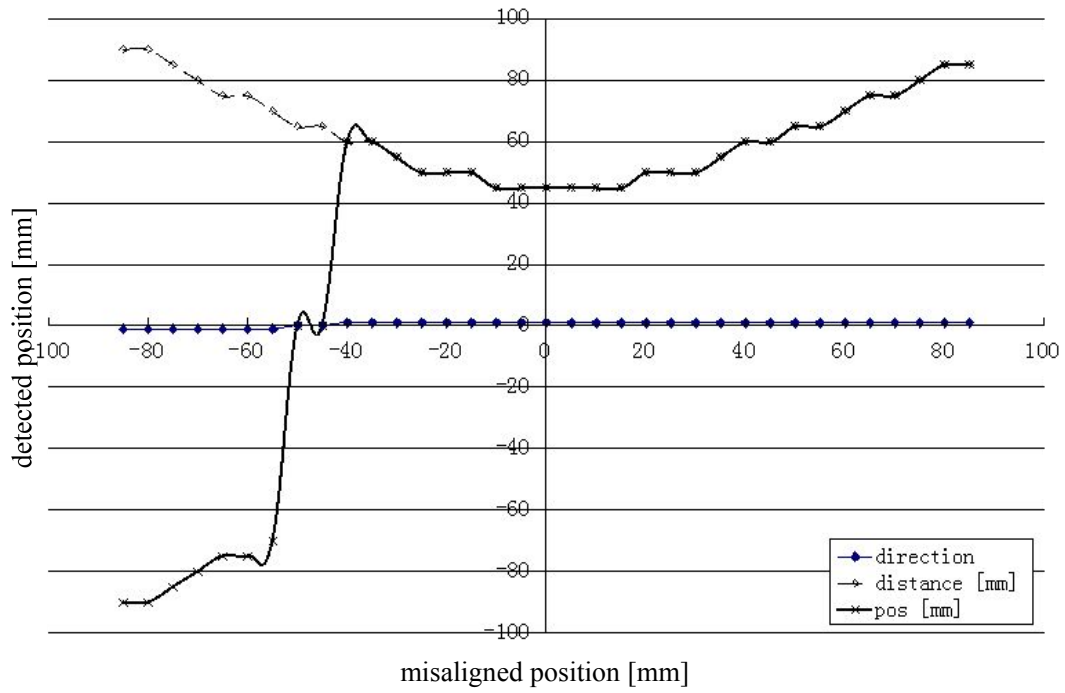
Fig_4.4.7 Position detected by using original curve at each misaligned position
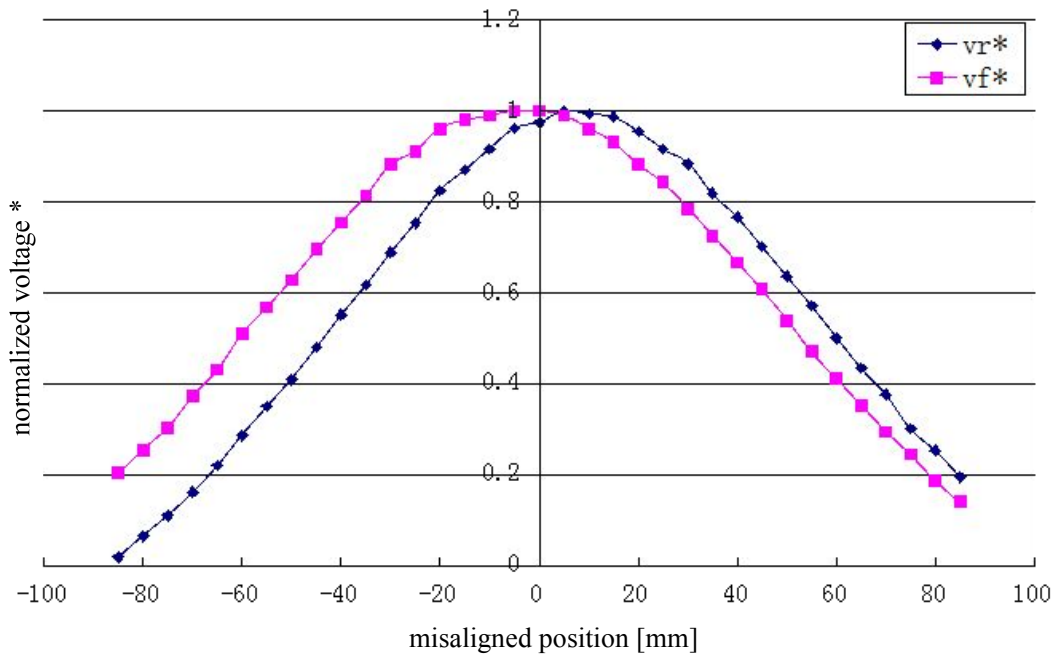
Fig_4.4.8 Normalized voltage-position characteristic curve

Fig_4.4.9 Position detected by using normalized curve at each misaligned position

(2) Position control

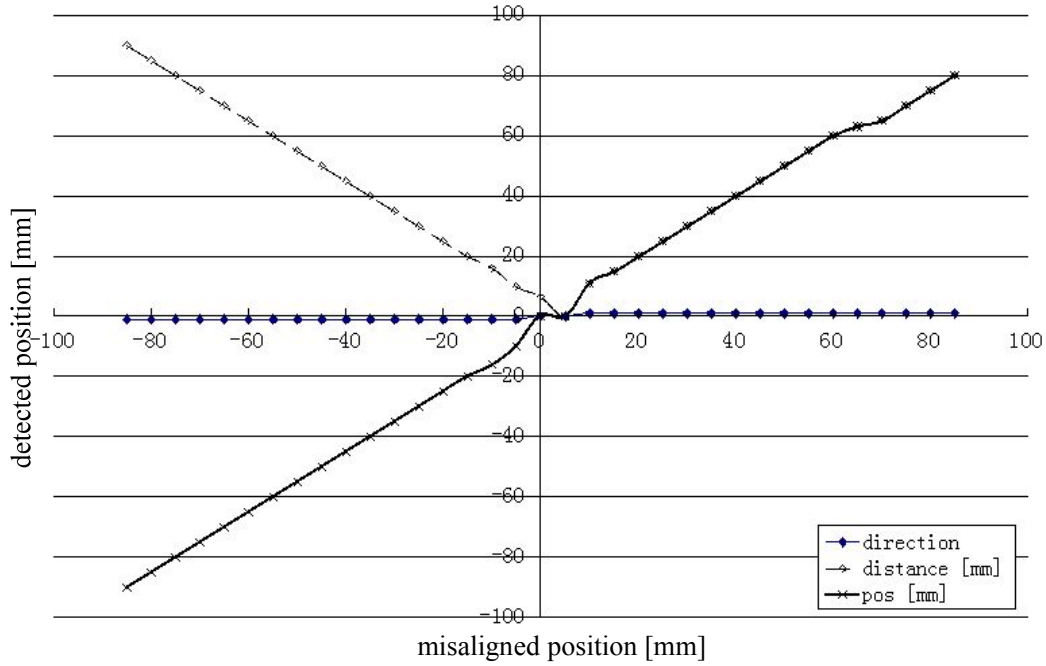Fig_4.4.10 and Fig_4.4.11 show the performance of position control. The starting position are still set as -80 mm and + 80 mm, as in case 1.

Similar to the result in case 1, the error of detected position are reduced by using proposed curve normalization method, and secondary coils are moved back to the aligned position with the error less than 5 mm. Therefore, the proposed method can satisfy the experiment objective, with the gap changes in the range of +100%, in this case.
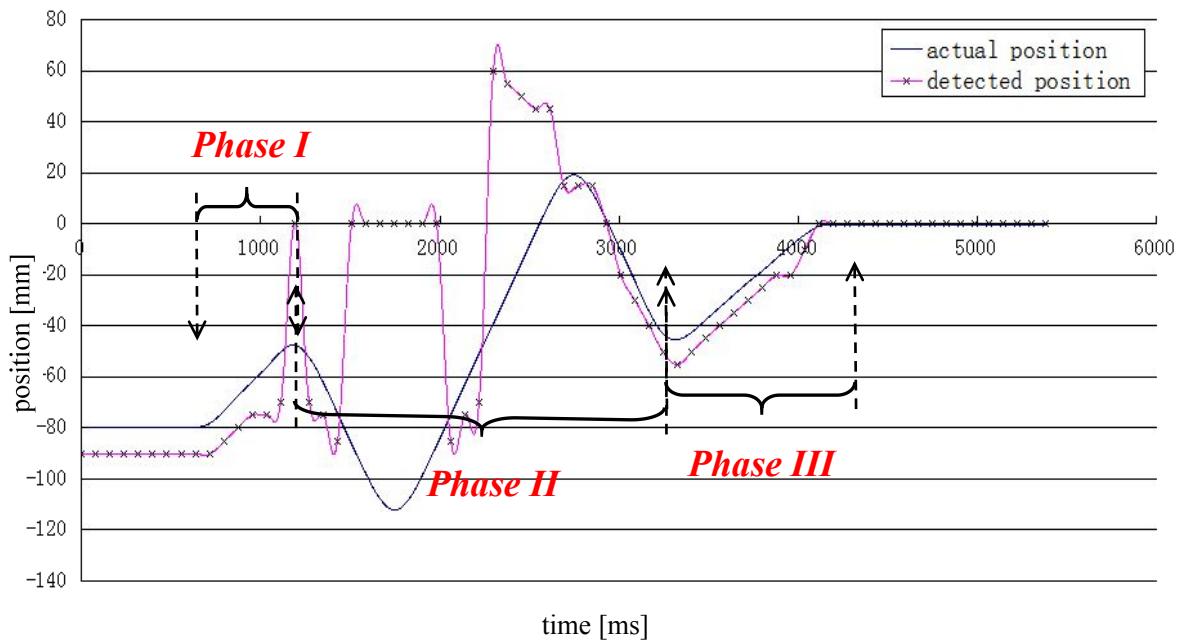
(a)
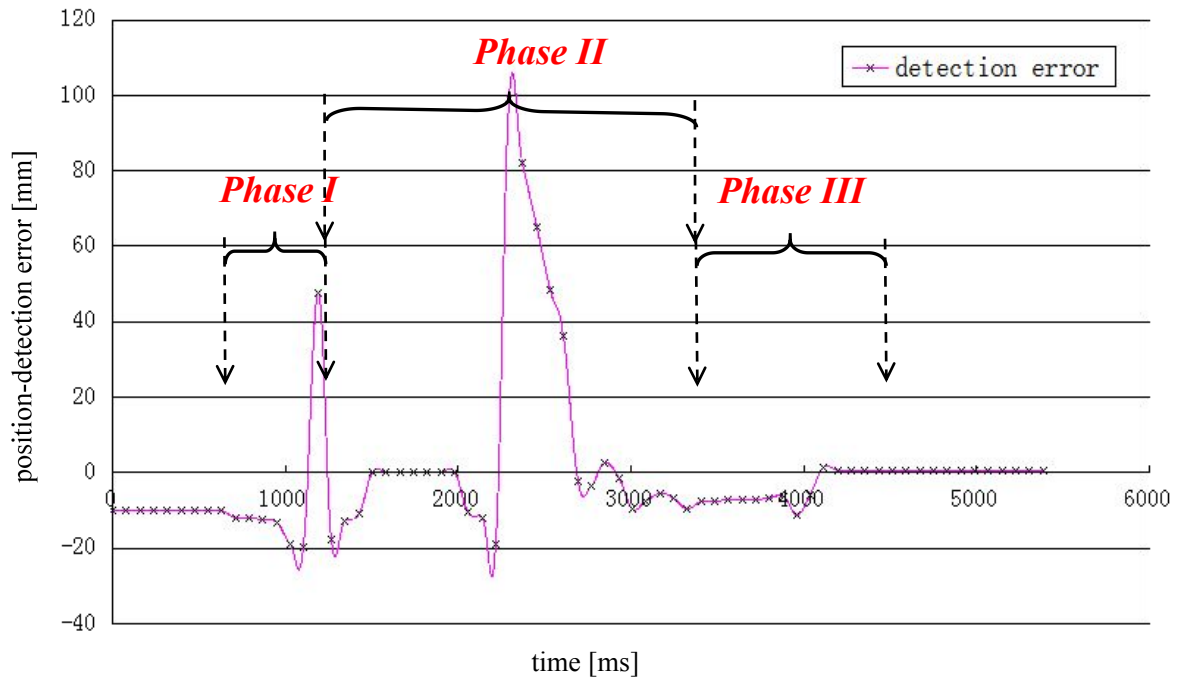
(b)

Fig_4.4.10 System performance--starts from -80 mm

(a) detected and actual position (b) detection error

Phase I: Move to inaccurate aligned position based on original voltage-position characteristic curve (close-loop)

Phase II: Scanning with fixed distance (open-loop)

Phase III: Move to accurate aligned position based on normalized curve(close-loop)

(a)
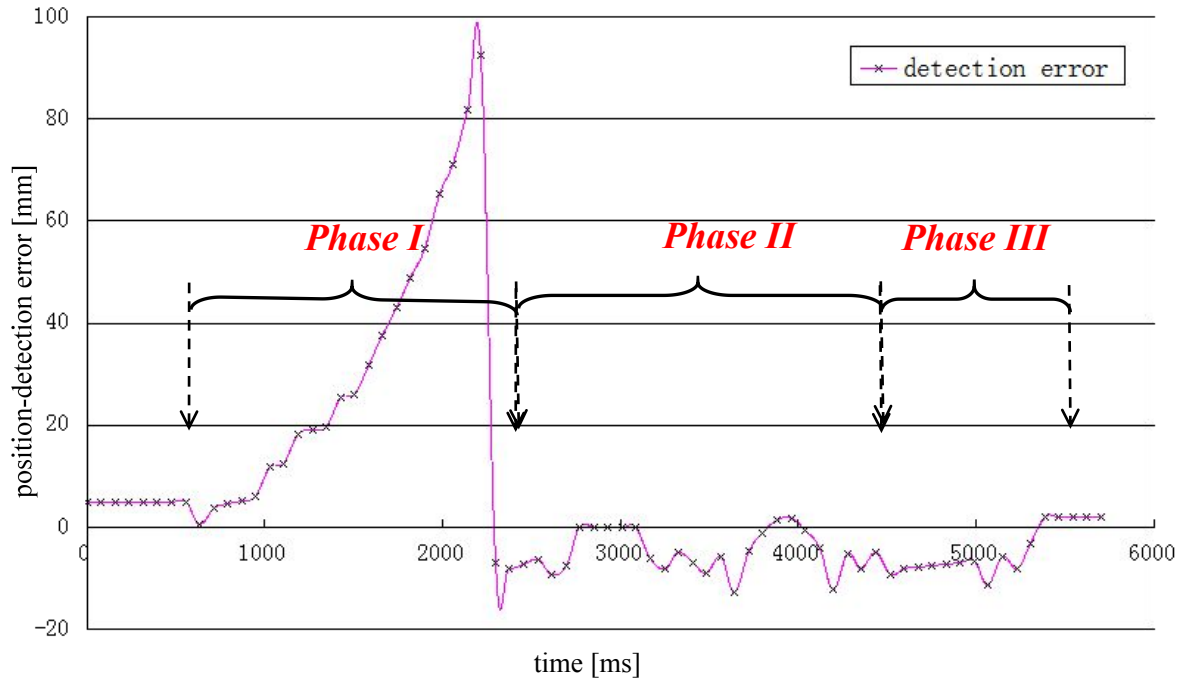
(b)

Fig_4.4.11 System performance--starts from +80 mm

(a) detected and actual position (b) detection error
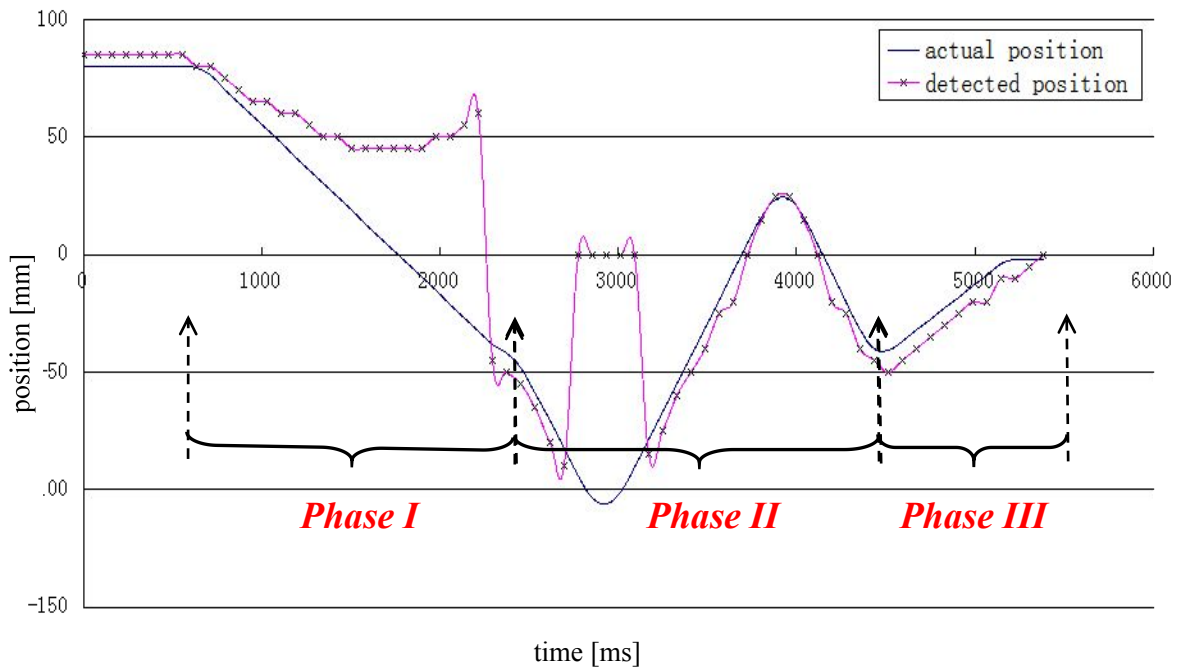
Phase I: Move to inaccurate aligned position based on original voltage-position
characteristic curve (close-loop)
Phase II: Scanning with fixed distance (open-loop)
Phase III: Move to accurate aligned position based on normalized curve (close-loop)

Position control in other cases are also executed, and results are shown in Tab_4.4.2. Maximum error, about 1 mm , is achieved when secondary side stops at +80 mm. Thus system robustness is also verified.

Tab_4.4.2 Performance at different position

Case No	Start position[mm]	Corrected position[mm]	Time [s]
1	-80	-0.91	3.51
2	-50	-0.72	3.09
3	-20	-1.33	3.41
4	20	-1.10	3.80
5	50	0.82	4.23
6	80	1.96	4.67

Chapter 5--Conclusions and Future Works

5.1 Conclusions

Two factors make misalignment a extremely serious problem in stationary wireless power transmission system for trains. One is the immovable coils, another is the inaccurate stopping position, these two factors always make the train suffer large misalignment and has limited solution towards it. In this paper, I proposed a coil moving system which can detect the misaligned position of coils and move them to the aligned position, thus the system tolerance to misalignment has been improved.

For coil position detection, to save the system cost and keep system reliable, a position sensorless detection method is proposed. Also, since vertical gap deviation often happens in wireless power transmission, a method to improve system robustness against gap deviation is also designed.

Both the sensorless position detection and gap deviation tolerance improving method are verified by experiment. As the result, the system is able to detect misalignment in the range of -50% ~+100% core length, and finally control coil misaligned position within (-5mm, +5 mm). By using the gap deviation tolerance improving method, the proposed system can reduced detection error form more than 50 mm to less than 5 mm, when the gap length changes within the range from -50% ~ +100% by vertical deviation. Finally, with such position control, charging power will be stable and efficiency will be ensured.

5.2 Future work

This paper proposed a method to detect and correct coil misaligned position for railways. The maximum detectable range in this system is about 50% core length, which means 400 mm if 800 mm length core is used to transfer high power. This detectable range can satisfy most situation of inaccurate stopping for Japanese railway, however, it still needs to be extended in case of extremely large misalignment cases.

Moreover, in this system, the execution time of position control is increased by scanning, and this maybe a drawback when this method is applied to railway system. When applying this system to real trains, on one hand, execution time will be increased due to longer execution range, on the other hand, it will be decreased by using faster actuator and optimized scanning algorithm. Thus the execution time should also be studied when applying it into real system.

Appendix A--Calculation of Actuator Cost

   Here we use the data of Yamamoto Line as an example to calculate the cost of actuators. In yamanote line, there are 29 stations and 52 trains in total, each train is consist of 10 vehicles [35].

Here are parameters for trains.
Number of Stations: Ns=29
Number of Trains: Nt=52
Number of Vehicles in One Train: Nv=10

If 4 coils are implemented for one vehicle, and one actuator can be used to move 4 coils:
Coils in one train: Nc=4*10=40
One actuator is used to move 4 coils

Then the necessity number of actuators can be calculated:
Case 1 Actuators are implemented on the train
Number of Actuators on one Train: Na_t=40/4=10
Total Number of Actuators: Ntotal=$Nat*Nt$=10*52=520

Case2 Actuators are implemented on the ground
Since the train runs at two directions, actuators should be implemented at both platform in the station, so actuator number should multiply 2.
Number of Actuators in one station: Na_s=(40/4)*2=20
Total Number of Actuators : $Ntotal$=20*29=580

As the result, if this system is applied to Yamamoto Line, cost will be less if actuators are implemented on trains. Also calculation is made based on Ginza Line[36], and the conclusion is the same.

Appendix B--Study of Resonance Circuit

Below is Fig_2.2.2, equivalent circuit of contectless transformer shown in chapter 2.
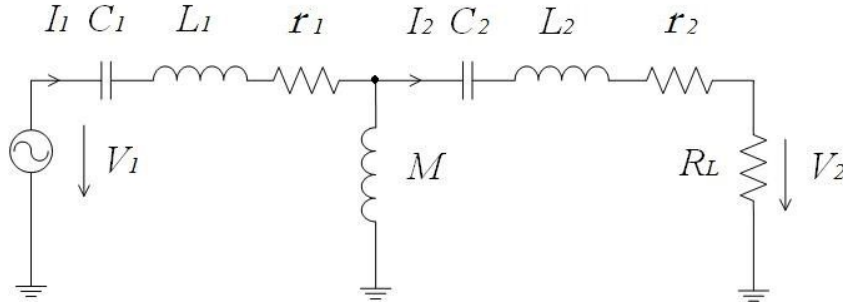
Fig_B.1 Equivalent circuit of contectless transformer

Now, if we make secondary side open-circuit, $I2$ will be 0 A. Eq(2-2) and eq (2-3) can be replaced by eq(B-1) and eq(B-2).

$$V_1 = j\omega(M + L_1)I_1 + I_1 r_1 - j\frac{1}{\omega C_1}I_1 \qquad (B-1)$$

$$j\omega M I_1 = V_2 \qquad (B-2)$$

Here $V2$ will be proportional to M, which signally decreases with the increase of misaligned distance, thus $V2$ can be used to obtain the misaligned distance. However, from the analysis in chapter 2, primary current $I1$ will be extremely large due to resonance at primary side, as in eq(B-3).

$$I_1 = \frac{V_1}{j\omega(L_1 + M) - j\frac{1}{\omega C_1} + r_1} \approx \frac{V_1}{r_1} \qquad (B-3)$$

This large current will generate overheated, in order to avoid this there are two possible ways. One way is using electronic switch to cut the capacitor when make position detection, but this will increase system cost and complexity. The other way is changing the frequency of power source, if we can make the system work at another frequency, the resonance will not happen. Details are shown below.

If frequency are increased by α times:

$$\omega_1 = \alpha\omega \qquad (B-4)$$

Primary inductance will also increase α times:

$$\omega_1(L_1 + M) = \alpha\omega(L_1 + M) \qquad (B-5)$$

Primary capacitance will be reduced to *1/α*.

$$\frac{1}{\omega_1 C_1} = \frac{1}{\alpha \omega C_1}$$

(B-6)

Thus the relation between primary inductance and capacitance will be:

$$\omega_1 (L_1 + M) = \alpha^2 \frac{1}{\omega_1 C_1}$$

(B-7)

As shown in eq(B-7), the effect of resonance will be eliminated if *α* is higher enough. From the simulation result, if *α* is selected to be 5, which means using 5 kHz to make position detection, the capacitive reactance will become 4% of inductive one, which means the effect of primary capacitor can be ignored. And finally we can get Fig_3.3.6 as a new equivalent circuit.

Appendix C--Experimental Test Bench
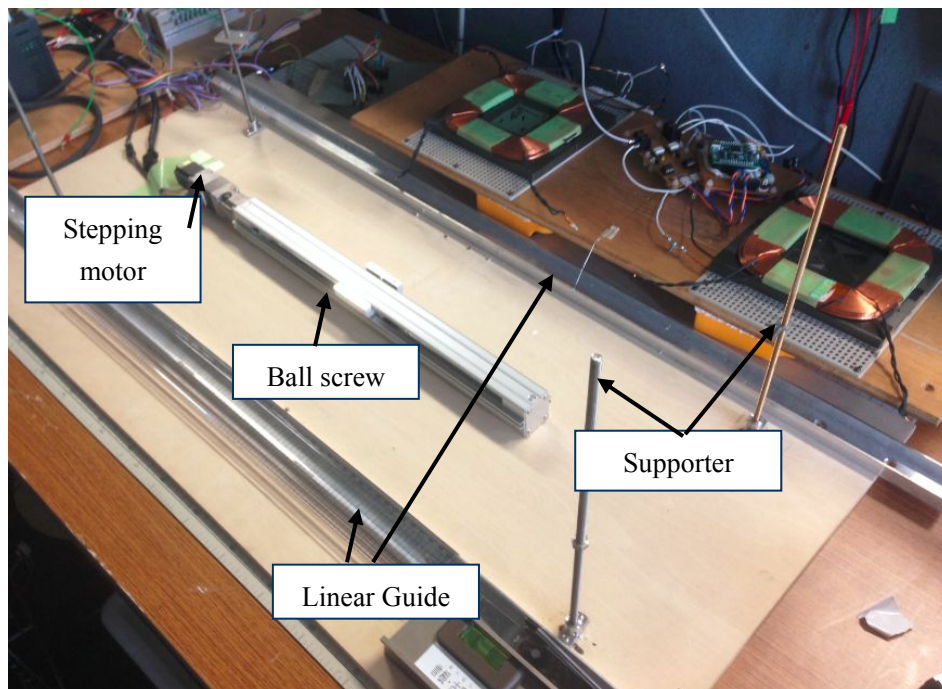
Fig_C.1 Stepping motor and ball screw
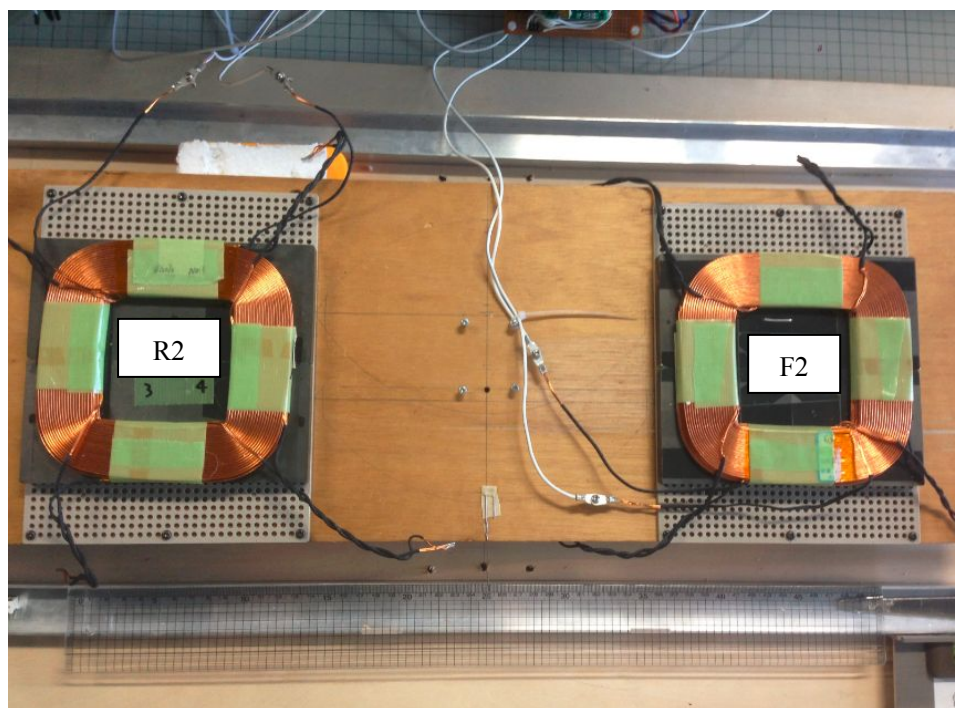
Fig_C.2 Secondary coils&cores
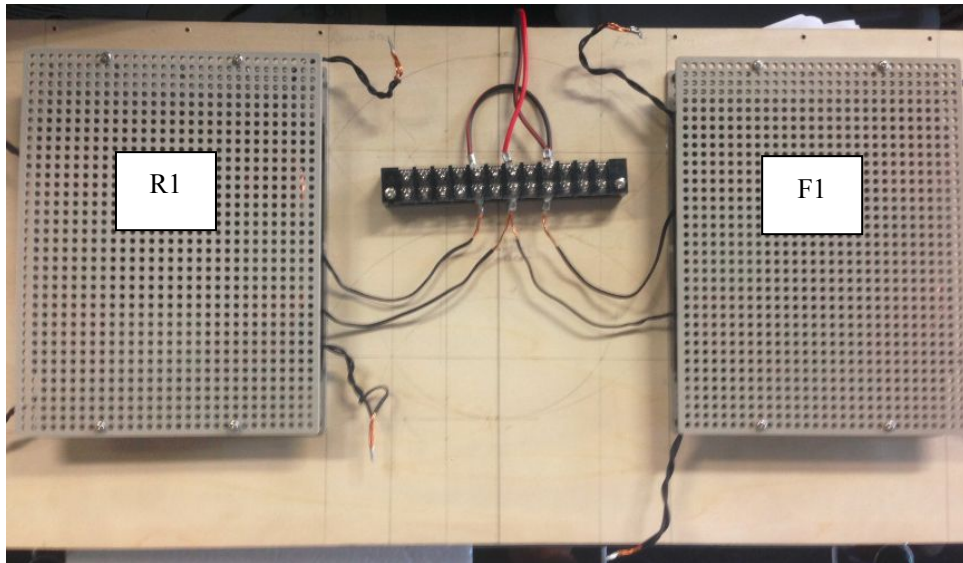
Fig_C.3 Primary coils&cores

Fig_C.4 Voltage sensor and micro controller

Table_B1. Component details

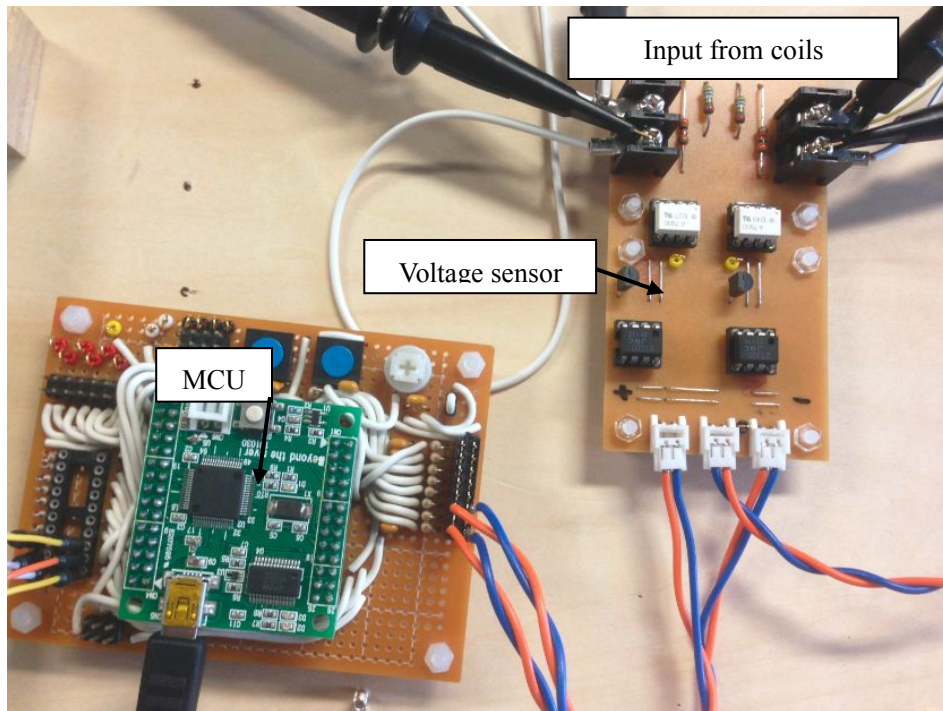| Part	Type	Producer
Ferrite Core	Mn-Zn PE22	TDK
Coil	Copper wire	DIY
Actuator	EAS2X-E030-ARMK-1	Orientalmotor
Voltage sensor	/	DIY
Micro Control Unit	SHZ 7125	Reneses

References

[1]. URL: http://blogs.yahoo.co.jp/tono19957814/62114585.html

[2]. URL: http://toyokeizai.net/articles/-/66456

[3]. Grant Covic and Jon Boys, "Inductive Power Transfer (IPT) Powering our Future", The University of Auckland, 2010.

[4]. Shinohara (2014) Wireless Power Transfer via Radiowaves, p. 11

[5]. Tesla, Nikola (May 20, 1891) "Experiments with Alternate Currents of Very High Frequency and Their Application to Methods of Artificial Illumination", lecture before the American Inst. of Electrical Engineers, Columbia College, New York. Reprinted as a book of the same name by. Wildside Press. 2006. ISBN 0809501627

[6]. Brown, William C. "The history of power transmission by radio waves". MTT-Trans. on Microwave Theory and Technique (Inst. of Electrical and Electronic Engineers) 32 (9): 1230–1234. (1984)

[7]. V. D. Doan, S. Watanabe and T. Koseki, "The design of an optimal running curve for train operation based on a novel parameterization method aiming to minimize the total energy consumption", Computers in Railways XIV, Vol.135, pp. 175 -190, June 2014.

[8]. Massa, A. Massa, G. Oliveri, F. Viani, and P. Rocca; Oliveri, Giacomo; Viani, Federico; Rocca, Paolo (June 2013)."Array designs for long-distance wireless power transmission – State-of-the-art and innovative solutions". Proceedings of the IEEE 101 (6): 1464–1481.

[9]. G. A. Landis, "Applications for Space Power by Laser Transmission," SPIE Optics, Electro-optics & Laser Conference, Los Angeles CA, 24–28 January 1994, Laser Power Beaming, SPIE Proceedings Vol. 2121, 252–255.

[10]. G. Landis, M. Stavnes, S. Oleson and J. Bozek, "Space Transfer With Ground-Based Laser/Electric Propulsion" (AIAA-92-3213) NASA Technical Memorandum TM-106060 (1992).

[11]. O. H. Stielau and G. A. Covic, "Design of loosely coupled inductive power transfer systems", Proceedings IEEE International Conference on Power System Technology, vol.1, pp. 8590, 2000.

[12]. G. A. Covic and J. T Boys, "Inductive power transfer," Proc. IEEE, vol. 101, no. 6, pp. 1276–1289, Jun. 2013.

[13]. Shinohara, Naoki, "Wireless power transmission progress for electric vehicle in Japan", Radio and Wireless Symposium (RWS), 2013 IEEE, pp.109,111, 20-23 Jan. 2013.

[14]. C. S. Wang, O. H. Stielau and G. A. Covic, "Design considerations for a contactless electric vehicle battery charger", IEEE transactions on Industrial Electronics, vol. 52, pp.1308-1314, 2005.

[15]. Peschiera,B. "Review of Inductive Power Transfer Technology for Electric and Plug-in Hybrid Electrical Vehicle", Industrial Electronics Society, IECON 2013 - 39th Annual Conference of the IEEE, pp.4672-4677, 10-13 Nov.2013

[16] J. Shin, B. Song, S. Lee, S. Shin, Y. Kim, G. Jung, and S. Jeon, "Contactless power transfer systems for on-line electric vehicle (OLEV)",in Proc. IEEE Int. Electric Veh. Conf., Mar. 2012, pp.1-4

[17]. Takehiro Imura, "Flexibility of Contactless Power Transfer Using Magnetic Coupling to Air Gap and Misalignment for EV", World Electric Vehicle Association Journal, Vol. 3, 2010

[18]. Palakon Kotchapansompote, Yafei Wang, Takehiro Imura, Hiroshi Fujimoto, Yoichi Hori, "Electric Vehicle Automatic Stop using Wireless Power Transfer Antennas", The 37th Annual Conference of the IEEE Industrial Electronics Society, pp. 3840-3845, 2011

[19]. Kiwon Hwang, Seonghwan, Seongkyu Kim, Yangbae Chun and Seungyoung Ahn, "Design of Wireless Power Transfer System for Railway Application", IJR International Journal of Railway,   Vol.5, No.4, pp. 167-174, Dec. 2012.

[20]. Seokhwan Lee, Guho Jung, Seungyong Shin,Yangsu Kim, Boyune Song, Jaegue Shin, Dongho Cho, "The optimal design of high-powered power supply modules for wireless power transferred train", Electrical   Systems for Aircraft, Railway and Ship Propulsion (ESARS), 2012, pp.1-4.

[21]. URL: http://primove.bombardier.com/applications/tram.html

[22]. Tim Dickson, "Wireless Electrification", Eighth International Hydrail Conference, (June. 2013)

[23]. S. Lukic and Z. Pantic, "Cutting the cord: Static and dynamic inductive wireless charging of electric vehicles," inElectrification Magazine, IEEE 2013, vol. 1, no. 1. pp. 57-64.

[24]. Su Y. Choi, Beom W. Gu, Seog Y. Jeong, and Chun T. Rim, "Ultraslim S-Type Power Supply Rails for Roadway-Powered Electric Vehicles," IEEE Transaction on Power Electronics, volume:30, issue: 11, pp.6456-6468, (2015)

[25]. Satoshi Kitazawa, "An Evaluation of Power Flow Control of the Power Conversion Circuit for Contactless Power Transformer System at the Coil Misalignment." IEEJ Transactions on Industry Applications Vol.133 No.5 pp.518-525

[26]. Nishimura, M.; Kawamura, A.; Kuroda, G.; Chi Zhu; Sato, E.K; "High Efficient Contact-less Power Transmission System for the High Speed Train" Power Electronics Specialists Conference, 2005. PESC '05. IEEE 36th, pp. 547- 553.

[27]. https://ja.wikipedia.org/wiki/停止位置目標

[28]. Aldhaher, S.; Luk, P.C.-K. and Whidborne, J.F., " Electronic Tuning of Misaligned Coils in Wireless Power Transfer Systems," IEEE Transactions on Power Electronics,Volume: 29, Issue: 11, Pages: 5975-5982, (2014)

[29]. T. Gerrits, D. C. J. Krop, L. Encica, and E. A. Lomonova, "Development of a linear position independent inductive energy transfer system" in Proc. Int. Mach. Drive Conference., 2011, pp.1-5.

[30]. Imura, T., " Equivalent circuit for repeater antenna for wireless power transfer via magnetic resonant coupling considering signed coupling," 2011 6th IEEE Conference on Industrial Electronics and Applications (ICIEA), Pages:1501-1506, (2011).

[31]. Cong Zheng, Rui Chen, Jih-Sheng Lai, "Design considerations to reduce gap variation andmisalignment effects for inductive power transfer system", Industrial Electronics Society, IECON 2014 - 40th Annual Conference of the IEEE, pp.1384-1390. (2014)

[32]. Negandra,G.R, Liang Chen, Covic G.a and Boys.J.T:"Detection of EVs on IPT highways". in Applied Power Electronics Conference and Exposition. 2014 Twenty-Ninth Annual IEEE, pp.1604-1611.(2014)

[33]. Hideki Matsuoka and Takafumi Koseki: "Evaluation of the change of the performance in an electromagnetic   induction   contactless   power   transformer   for   railways   by   the   coil

misalignment and the gap length", J-RAIL2013, S9-12, pp317-320, (2013-12) (in Japanese)

[34]. T.Maruyama. "Study on the Design Method of the Light Weight Coils for a High Power Contactless Power Transfer Systems". Master thesis of Chiba University.(2013)

[35]. https://ja.wikipedia.org/wiki/山手線

[36]. https://ja.wikipedia.org/wiki/東京メトロ銀座線

List of Publications

[1]. Sigang Luo, Hideki Matsuoka, Takafumi Koseki: "Position-Sensorless Detection of Coil Misalignment for Wireless Static Power Charging of Electric Trains," IEEJ.TER-15-025, pp. 43-48, (May,2015).

[2]. Sigang Luo, Yasuhiro Takada, Takafumi Koseki, Tatsuhito Saito, Febry Pandu Wijaya, Keiichiro Kondo: "Experiment Verification of Sensorless Coil Position Control System and its Gap Deviation Tolerance Improvement Method in Wireless Power Transmission System of Electrical Trains," IEEJ.VT-15-022, (Sept, 2015),(in preparation).